A STUDY OF THE EFFECTS OF A LONGITUDINAL, INTERIOR PLATE ON THE FREE VIBRATIONS OF CIRCULAR CYLINDRICAL SHELLS

By

MICHAEL RALPH PETERSON

Bachelor of Science in Mechanical Engineering
University of New Mexico
Albuquerque, New Mexico
1967

Master of Science
University of New Mexico
Albuquerque, New Mexico
1969

Submitted to the Faculty of the Graduate College
of the Oklahoma State University
in partial fulfillment of the requirements
for the Degree of
DOCTOR OF PHILOSOPHY
December, 1973

A STUDY OF THE EFFECTS OF A LONGITUDINAL, INTERIOR PLATE ON THE FREE VIBRATIONS OF CIRCULAR CYLINDRICAL SHELLS

Thesis Approved:

Donald E. Boyd
Thesis Adviser

James E Bose

R L Lowery

R Kumnick

W M Dunham
Dean of the Graduate College

ACKNOWLEDGMENTS

The aid of those who helped during this study is gratefully acknowledged. I would like to express my appreciation to Dr. Donald E. Boyd, my major adviser, for his advice, instruction and encouragement during my graduate study. My thanks are extended to Drs. R. L. Lowery, J. E. Bose, and R. K. Munshi for serving on my doctoral committee.

My appreciation is expressed also to Robert Brugh and Mahabaliraja for their suggestions, encouragement, and interesting discussions. I thank Charlene Fries for assisting in the preparation of the final manuscript.

The School of Mechanical and Aerospace Engineering provided a Graduate Assistantship which helped make my graduate study possible.

TABLE OF CONTENTS

LIST OF TABLES

LIST OF FIGURES

LIST OF SYMBOLS

[B]	matrix relating strains to generalized coordinates
b	half width of plate
[C]	constraint matrix
D	bending rigidity
[D]	matrix of elastic constants, relating stress to strain
E	modulus of elasticity
[E]	transformation matrix which transforms the set of all generalized coordinates into an independent subset
f	frequency in hertz
[G]	matrix relating strain to displacement
H_1 to H_{11}	integrals of the plate transverse displacement functions
I_1 to I_5	integrals of the longitudinal displacement functions
J_1 to J_{15}	integrals of the shell circumferential displacement functions
K	extensional rigidity
[K]	stiffness matrix
[K*]	stiffness matrix of plate and shell in unconstrained coordinates
L	length of partitioned shell
$\bar{M}$	number of values of m in the displacement series
[M]	mass matrix
[M*]	mass matrix of shell and plate in unconstrained coordinates

m	subscript referring to longitudinal terms in the displacement series
$\bar{m}$	number of longitudinal half waves in a vibration mode of the partitioned shell
m^*	highest value of m in the displacement series
$\bar{N}$	number of values of n in the displacement series
$[N]$	transformation matrix between generalized coordinates and displacements
n	subscript referring to circumferential or transverse terms in the displacement series
$\bar{n}$	number of shell circumferential waves in a vibration mode
n^*	highest value of n in the displacement series
$\{q\}$	vector of generalized coordinates
$\{q_1\}$	vector of independent set of generalized coordinates
$\{q_2\}$	vector of dependent set of generalized coordinates
R	radius of shell
r	radial coordinate
T	kinetic energy
t	thickness, time
U	strain energy
U^P_{mn}, V^P_{mn}, W^P_{mn}	generalized coordinates of the plate
U^S_{mn}, V^S_{mn}, W^S_{mn}	generalized coordinates of the shell
u_s, v_s, w_s	middle surface displacements of the shell in the x, θ, z_s directions, respectively
u_p, v_p, w_p	middle surface displacements of the plate in the x, y, z_p directions, respectively
$\{\tilde{u}\}$	vector of u, v, w displacements for shell or plate
X_{um}, X_{vm}, X_{wm}	m^{th} longitudinal function in the assumed displacement series
x, y, z_p	spatial coordinates of the plate
x, θ, z_s	spatial coordinates of the shell

α_m, β_m	constants appearing in the beam mode functions
δ	symbol indicating variation
$\{\varepsilon\}$	vector of strains and curvatures
θ_o	value of θ at which the joint between the plate and shell is located
Θ_{un}, Θ_{vn}, Θ_{wn}	n^{th} circumferential function in the assumed displacement series
λ	eigenvalue
$\{\lambda\}$	vector of Lagrange multipliers
ν	Poisson's ratio
ξ_{un}, ξ_{vn}, ξ_{wn}	n^{th} plate transverse function in the series representing the u_p, v_p, w_p displacements, respectively
ρ	mass density per unit area
$\{\sigma\}$	vector of stress resultants
ϕ_x^p, ϕ_y^p, ϕ_z^p	rotations of a point in the plate middle surface about the plate x, y, z_p axes
ϕ_x^s, ϕ_θ^s, ϕ_z^s	rotations of a point in the shell middle surface about the shell x, θ, z_s axes
ψ_{un}, ψ_{vn}, ψ	n^{th} shell circumferential functions in the series representing u_s, v_s, w_s displacements, respectively
ω	circular frequency
Ω	nondimensional frequency, $\Omega^2 = \frac{\omega^2 R^2 \rho(1-\nu^2)}{E}$

Subscripts

m, n	refer to terms in displacement series
p	refers to plate
s	refers to shell

Notes

(1) a dot above a quantity denotes the time derivative

(2) a prime superscript on a function denotes differentiation with respect to the independent variable

(3) a superscript T indicates the transpose of a matrix or vector

CHAPTER I

INTRODUCTION

Much information is available on the free vibration characteristics of circular cylindrical shells. A knowledge of the natural frequencies and characteristic modes of cylindrical shells and how they change with the geometric parameters of the shell is useful for the design of shell structures. However, many structures for aerospace, marine, and industrial applications have the basic form of a cylindrical shell partitioned by a longitudinal plate. For example, a section of an aircraft fuselage with a floor structure may be idealized as a partitioned shell. The results of vibration studies of unpartitioned cylindrical shells will not necessarily apply to a partitioned shell, and no such results on partitioned shells are available. Thus, a need exists for information about the vibrations of a partitioned shell.

The general purpose of this study is to investigate the free vibrational behavior of a partitioned cylindrical shell. The specific objectives are:

1. To develop a method and associated computer program for calculating the natural frequencies and mode shapes of circular cylindrical shells with single longitudinal partitioning plates.

2. To determine how the frequencies and mode shapes of the system differ for a rigid and hinged joint between the shell and plate.

3. To study the effects of the thickness and position of the plate on the frequencies and mode shapes of the system.

Background

The literature contains results of many analytical and experimental studies of the vibrations of circular cylindrical shells. An important example, which first explained some of the characteristics of the vibrations of cylindrical shells, was made by Arnold and Warburton (1). They calculated the frequencies of a freely supported cylinder by using a Rayleigh-Ritz approach and verified the calculated results experimentally.

Many methods of analysis have been used to study the vibrations of cylindrical shells. Closed-form solutions have been obtained by various methods for some problems. Simplifying assumptions, which are justifiable for some problems, have yielded approximate solutions. Techniques such as the Galerkin, finite difference, and finite element methods have also been used (2, 3, 4).

Problems involving complications to the cylindrical shell usually require the use of numerical methods and a digital computer. The Rayleigh-Ritz method has been used to solve for the natural frequencies and modes of noncircular shells, and ring and stringer-stiffened shells, both circular and noncircular (5, 6, 7, 8). The stiffening members in these analyses were treated by expressing their displacements in terms of the shell middle-surface displacements by means of compatibility equations. The problem is thus formulated entirely in terms of the shell displacements.

A few papers treat partitions or interior structures in shells. Junger (9) considers rigid circular bulkheads (planes normal to cylinder axes) dividing circular cylindrical shells. Basdekas and Chi (10) present a variation of the Rayleigh-Ritz method for the analysis of ring stiffened cylindrical shells in which the stiffening rings may have cross members in the plane of the ring. Klein (11) used the finite element method to analyze a particular axisymmetric shell with spherical internal bulkheads. Argyris (12, 13) describes the finite element force method for the static and dynamic analyses of aircraft fuselages with floors, but presents no results. No results from studies of longitudinally partitioned shells have been found in a search of the literature.

Regions of a structure can be considered separately in an analysis if constraint equations are used to enforce compatibility between them. This basic approach has been used with various methods of analysis. Some shell problems for which it has been used are: ring and stringer stiffened shells; cylindrical panel segments joined together to form a shell with a cross section made up of circular arcs for a buckling analysis; and a cone joined to a cylinder (14, 15, 16). Modal coupling methods, which are designed to synthesize the modes of a structure from the modes of its components, also make use of this approach (17, 18).

In the usual Rayleigh-Ritz method, displacement functions are assumed for the shell in the form of series with undetermined coefficients, each term of which satisfies the external and internal kinematic compatibility conditions. By using Hamilton's principle or an equivalent, a set of equations of motion for the system in terms of the coefficients of the displacement series is obtained. In the extended Rayleigh-Ritz method, the assumed displacement functions need not satisfy

the compatibility conditions; instead, these conditions are enforced by constraint equations. Budiansky and Hu (19, 20) first applied this method to satisfy the boundary conditions in plate buckling problems. Webster (21, 22) used the method to join a spherical end cap to a cylinder, and to enforce boundary conditions in a study of curved panels.

Approach to the Problem

The first objective of this study is to develop a method and associated computer program for the analysis of cylindrical shells with single longitudinal partitioning plates. The Rayleigh-Ritz method is used as the basis for this analysis. The basic Rayleigh-Ritz method has proved very successful for analysis of shells with complications such as ring and stringer stiffening, and it has advantages over other methods such as the finite difference and finite element methods. The finite element method usually requires a large number of degrees of freedom. Webster (21) has compared the extended Rayleigh-Ritz method using power series displacement functions with the finite element method for a plate problem. He concluded that fewer degrees of freedom were necessary for satisfactory results with the extended Rayleigh-Ritz method. The number of degrees of freedom is important for vibration problems, because the cost of the computer solution of the resulting eigenvalue problem rises sharply as the number of degrees of freedom increases. Also, in contrast to the Rayleigh-Ritz method, the finite element model is tedious to construct and new models must be generated to test convergence or to change the geometric parameters of the problem. Thus, the Rayleigh-Ritz method is an efficient method for this study, in which many problems with varying geometric parameters must be considered.

The equations of motion developed in this study for a partitioned shell are based on Love's shell theory and the classical plate theory. The assumed displacement functions in the Rayleigh-Ritz method are assumed for the plate and shell separately. Compatibility between the shell and plate is enforced with constraint equations. The method of analysis is presented in Chapter II.

A computer program was written to perform the calculations. It was used to study the effects of the joint condition, and the thickness and position of the plate on the frequencies and mode shapes of the system. These results are presented in Chapter III. Conclusions about the vibrational characteristics of partitioned shells are given in Chapter IV.

CHAPTER II

METHOD OF ANALYSIS

Development of the Equations of Motion

The geometry of a typical circular cylindrical shell with a longitudinal partitioning plate and the coordinate systems associated with it are shown by Figure 1. The extended Rayleigh-Ritz method is used to reduce the shell and plate system to a system having a finite number of degrees of freedom. This is done by assuming separate displacement functions for the plate and shell, each in the form of finite series with undetermined coefficients. Constraint equations are used to enforce compatibility of displacements and rotations between the plate and shell. Once the problem has been discretized in this manner, the application of Hamilton's principle will lead to the equations of motion of the system in the form of an algebraic eigenvalue problem in terms of the undetermined coefficients in the series of assumed functions. The undetermined coefficients are the generalized coordinates of the system.

For a free vibration problem, Hamilton's principle can be stated as

$$\delta A = \delta \int_{t_1}^{t_2} (T-U)dt = 0 \qquad (2.1)$$

where T and U are the kinetic and strain energies, respectively, expressed in terms of independent coordinates and t_1 and t_2 are two arbitrary points in time.

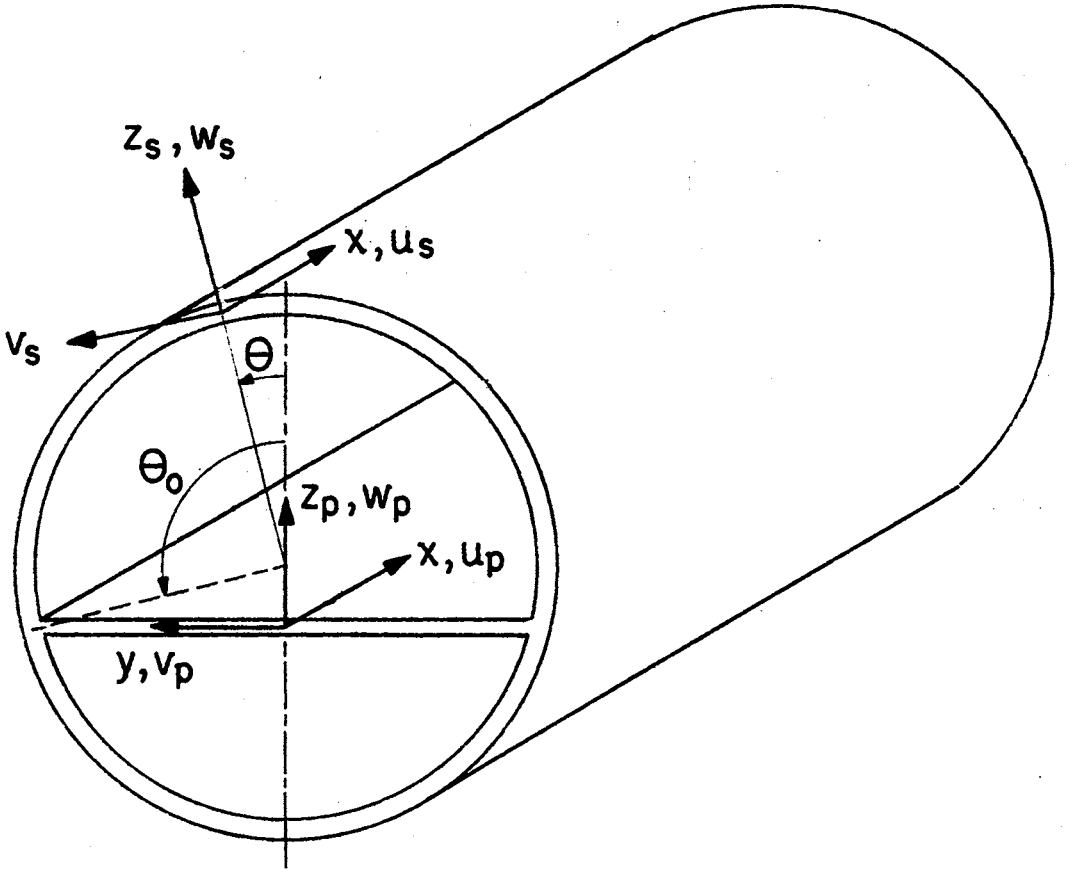

Figure 1. Geometry of a Circular Cylindrical Shell With a Longitudinal Partitioning Plate

Displacement functions of the following form will be assumed:

$$u_s = \sum_{m=0}^{m^*} \sum_{n=0}^{n^*} U_{mn} X_{um}(x) \Theta_{um}(\theta)$$

$$v_s = \sum_{m=0}^{m^*} \sum_{n=0}^{n^*} V_{mn} X_{vm}(x) \Theta_{vn}(\theta) \qquad (2.2)$$

$$w_s = \sum_{m=0}^{m^*} \sum_{n=0}^{n^*} W_{mn} X_{wm}(x) \Theta_{wn}(\theta)$$

These displacement functions may be written in the matrix form

$$\begin{Bmatrix} u_s \\ v_s \\ w_s \end{Bmatrix} = [N_s] \{q_s\} \qquad (2.3)$$

where $[N_s]$ is a matrix of size 3 x $3\bar{M}\bar{N}$ and $\{q_s\}$, a vector of the generalized coordinates of the shell, is given by

$$\{q_s\} = \begin{Bmatrix} \bar{u}_s \\ \bar{v}_s \\ \bar{w}_s \end{Bmatrix}$$

wherein

$$\{\bar{u}_s\} = \begin{Bmatrix} U_{oo} \\ U_{o1} \\ \cdot \\ \cdot \\ \cdot \\ U_{on^*} \\ U_{1n^*} \\ \cdot \\ \cdot \\ \cdot \\ U_{m^*n^*} \end{Bmatrix}, \{\bar{v}_s\} = \begin{Bmatrix} V_{oo} \\ V_{o1} \\ \cdot \\ \cdot \\ \cdot \\ V_{on^*} \\ V_{1n^*} \\ \cdot \\ \cdot \\ \cdot \\ V_{m^*n^*} \end{Bmatrix}, \{\bar{w}_s\} = \begin{Bmatrix} W_{oo} \\ W_{o1} \\ \cdot \\ \cdot \\ \cdot \\ W_{on^*} \\ W_{1n^*} \\ \cdot \\ \cdot \\ \cdot \\ W_{m^*n^*} \end{Bmatrix} \qquad (2.4)$$

The displacements of the plate can also be expressed in the form of Equation (2.2) and in the matrix form

$$\begin{Bmatrix} u_p \\ v_p \\ w_p \end{Bmatrix} = [N_p] \{q_p\} \tag{2.5}$$

in which the elements of $\{q_p\}$ are the generalized coordinates of the plate, arranged in the same manner as the elements of $\{q_s\}$.

The strain and kinetic energies of the shell and plate can be expressed in terms of the generalized coordinates by using the strain-displacement relations of shell and plate theory and the material constitutive relations. For either the shell or plate the strain energy can be expressed as

$$U = \frac{1}{2} \int_S \{\sigma\}^T \{\varepsilon\} \, dS \tag{2.6}$$

where $\{\sigma\}$ is a vector of stress resultants and $\{\varepsilon\}$ is a vector of strains and curvatures for the plate or shell. Since the following development is the same for the plate and shell through Equation (2.14), subscripts on the variables will be omitted with the understanding that each of the equations applies to either the shell or plate.

For a linearly elastic material,

$$\{\sigma\} = [D] \{\varepsilon\} \tag{2.7}$$

in which [D] is a matrix of elastic constants. The strain-displacement relations, obtained from shell and plate theory, have the form

$$\{\varepsilon\} = [G] \{\tilde{u}\}, \text{ where } \{\tilde{u}\} = \begin{Bmatrix} u \\ v \\ w \end{Bmatrix}. \tag{2.8}$$

In this analysis, the strain-displacement relations of Love's shell theory and the classical plate theory are used. They are presented in Appendixes A and B. Substitution of Equations (2.7) and (2.8) into (2.6) yields the following result:

$$U = \frac{1}{2}\int_S ([G]\{\tilde{u}\})^T\,[D]\,[G]\,\{\tilde{u}\}\,dS \tag{2.9}$$

The displacements $\{\tilde{u}\}$ are related to the generalized coordinates by

$$\{\tilde{u}\} = [N]\{q\}.$$

Then, in terms of $\{q\}$, Equation (2.9) is

$$U = \frac{1}{2}\int_S ([G][N]\{q\})^T\,[D]\,[G]\,[N]\,\{q\}\,dS.$$

By defining $[B] = [G]\,[N]$, this becomes

$$U = \frac{1}{2}\int_S \{q\}^T\,[B]^T\,[D]\,[B]\,\{q\}\,dS,$$

or

$$U = \frac{1}{2}\{q\}^T[K]\{q\} \tag{2.10}$$

where

$$[K] = \int_S [B]^T[D][B]\,dS \tag{2.11}$$

is defined as the stiffness matrix of the shell or plate.

The kinetic energy of the plate or shell is

$$T = \frac{1}{2}\int_S \rho\{\dot{\tilde{u}}\}^T\{\dot{\tilde{u}}\}\,dS. \tag{2.12}$$

The kinetic energy in terms of the generalized coordinates can be expressed as

$$T = \frac{1}{2}\int_S \rho\{\dot{q}\}^T[N]^T[N]\{\dot{q}\}\,dS.$$

The mass matrix is defined as

$$M = \int_S \rho[N]^T\,[N]\,dS. \tag{2.13}$$

Then

$$T = \frac{1}{2} \{\dot{q}\}^T [M] \{\dot{q}\}. \tag{2.14}$$

The elements of the mass and stiffness matrices of the shell and plate are given in Appendixes A and B.

The kinetic energies of the shell and plate are

$$T_s = \frac{1}{2} \{\dot{q}_s\}^T [M_s] \{\dot{q}_s\}$$

and

$$T_p = \frac{1}{2} \{\dot{q}_p\}^T [M_p] \{\dot{q}_p\}$$

where subscripts referring to the shell and plate are now included. The total kinetic energy for the system is the sum of the kinetic energies of the shell and plate: $T = T_s + T_p$.

The total kinetic energy can be expressed in the following form:

$$T = \frac{1}{2} \begin{Bmatrix} \dot{q}_s \\ \dot{q}_s \end{Bmatrix}^T \begin{bmatrix} M_s & 0 \\ 0 & M_p \end{bmatrix} \begin{Bmatrix} \dot{q}_s \\ \dot{q}_p \end{Bmatrix} = \frac{1}{2} \{\dot{q}\}^T [M^*] \{\dot{q}\} \tag{2.15}$$

in which

$$\{q\} = \begin{Bmatrix} q_s \\ q_p \end{Bmatrix}$$

is the combined vector of all the generalized coordinates of the shell and plate.

Likewise, the strain energies for the shell and plate are

$$U_s = \frac{1}{2} \{q_s\}^T [K_s] \{q_s\} \text{ and } U_p = \frac{1}{2} \{q_p\}^T [K_p] \{q_p\}.$$

Hence, the total strain energy is

$$U = U_s + U_p = \frac{1}{2} \begin{Bmatrix} q_s \\ q_p \end{Bmatrix}^T \begin{bmatrix} K_s & 0 \\ 0 & K_p \end{bmatrix} \begin{Bmatrix} q_s \\ q_p \end{Bmatrix}, \tag{2.16}$$

or

$$U = \frac{1}{2} \{q^T\}[K^*]\{q\}.$$

The matrices [M*] and [K*] are the mass and stiffness matrices for the unassembled system consisting of the plate and shell.

The components of the coordinate vector {q} are not independent because constraint equations must be introduced to insure displacement compatibility at the interface between the plate and shell. The equations expressing this compatibility can be written in terms of the generalized coordinates in the following matrix form:

$$[C]\{q\} = \{0\}. \tag{2.17}$$

Since Hamilton's principle as given by Equation (2.1) requires independent coordinates, it must be modified to include the constraint equations. This can be done by introducing a vector of Lagrange multipliers, {λ}, and adjoining the constraint equations to the integrand, i.e.

$$\delta A = \delta \int_{t_1}^{t_2} (T-U-\{\lambda\}^T[C]\{q\})\, dt = 0. \tag{2.18}$$

This can also be written as

$$\delta A = \int_{t_1}^{t_2} (\delta T-\delta U-\{\delta\lambda\}^T[C]\{q\} - \{\lambda\}^T[C]\{\delta q\})\, dt = 0. \tag{2.19}$$

Because $\{\lambda\}^T[C]\{\delta q\}$ is a scalar, $\{\lambda\}^T[C]\{\delta q\} = \{\delta q\}^T[C]^T\{\lambda\}$. Taking the variations of the expressions for the kinetic and potential energies and using them in Equation (2.19), the following is obtained:

$$\delta A = \int_{t_1}^{t_2} (-\{\delta q\}^T[M^*]\{\ddot{q}\} - \{\delta q\}^T[K^*]\{q\} - \{\delta\lambda\}^T[C]\{q\}$$

$$- \{\delta q\}^T[C]^T\{\lambda\})dt = 0$$

$$= -\int_{t_1}^{t_2} [\{q\}^T([M^*]\{\ddot{q}\} + [K^*]\{q\} + [C]^T\{\lambda\})$$

$$+ \{\delta q\}^T[C]\{q\}]dt = 0.$$

The elements of $\{\lambda\}$ are arbitrary, so they will be chosen to satisfy

$$[M^*]\ \{\ddot{q}\} + [K^*]\ \{q\} + [C]^T\ \{\lambda\} = \{0\}$$

Then $\{\delta\lambda\}^T$ cannot be zero, so $[C]\ \{q\} = \{0\}$.

Thus the equations of motion and constraint for the system are:

$$[M^*]\ \{\ddot{q}\} + [K^*]\ \{q\} + [C]^T\ \{\lambda\} = \{0\} \tag{2.20}$$

$$[C]\ \{q\} = \{0\}.$$

These equations can be written in another form, which is more convenient for their solution.

If $\{q\}$ is partitioned into a set of independent coordinates $\{q_1\}$ and dependent coordinates $\{q_2\}$, then the constraint equations can be written

$$\left[C_1 \vdots C_2\right] \begin{Bmatrix} q_1 \\ q_2 \end{Bmatrix} = \{0\} \tag{2.21}$$

The dependent coordinates and Lagrange multipliers can be algebraically eliminated from Equation (2.20), which take the form:

$$[M]\ \{\ddot{q}_1\} + [K]\ \{q_1\} = \{0\} \tag{2.22}$$

in which

$$[M] = [E]^T\ [M^*]\ [E],\ [K] = [E]^T\ [K^*]\ [E] \tag{2.23}$$

where

$$[E] = \begin{bmatrix} I \\ \hline [C_2]^{-1}\ [C_1] \end{bmatrix} \tag{2.24}$$

The matrix [E] defines a linear transformation between the original dependent set of coordinates {q} and the independent subset $\{q_1\}$. For harmonic motion, Equation (2.22) takes the form:

$$([K] - \omega^2 [M]) \{q_1\} = \{0\}. \tag{2.25}$$

This is an algebraic eigenvalue problem in which the eigenvalues are proportional to the natural frequencies and the eigenvectors describe the mode shapes in terms of the generalized coordinates.

Displacement Functions

The displacement functions are assumed to be finite series, each term of which is the product of a function of the longitudinal coordinate, a function of the shell circumferential coordinate or plate transverse coordinate, and the generalized coordinate. The following series are used for the shell:

$$\begin{aligned}
u_s &= \sum_{m=0}^{m^*} \sum_{n=0}^{n^*} U^s_{mn} X_{um}(x) \psi_{un}(\theta) \\
v_s &= \sum_{m=0}^{m^*} \sum_{n=0}^{n^*} V^s_{mn} X_{vm}(x) \psi_{vn}(\theta) \\
w_s &= \sum_{m=0}^{m^*} \sum_{n=0}^{n^*} W^s_{mn} X_{wm}(x) \psi_{wn}(\theta).
\end{aligned} \tag{2.26}$$

For the plate, the series are:

$$u_p = \sum_{m=0}^{m^*} \sum_{n=0}^{n^*} U^p_{mn} X_{um}(x) \xi_{un}(y)$$

$$v_p = \sum_{m=0}^{m^*} \sum_{n=0}^{n^*} V_{mn}^p \, X_{vm}(x) \, \xi_{vn}(y) \tag{2.27}$$

$$w_p = \sum_{m=0}^{m^*} \sum_{n=0}^{n^*} W_{mn}^p \, X_{wm}(x) \, \xi_{wn}(y)$$

The longitudinal functions X(x) are the same for the plate and the shell. These functions are expressed in terms of a single function $\phi(x)$, in the following manner:

$$\begin{aligned} X_{um} &= \phi_m'(x) \\ X_{vm} &= \phi_m(x) \\ X_{wm} &= \phi_m(x) \end{aligned} \tag{2.28}$$

The functions $\phi_m(x)$ are the vibration mode functions of a uniform beam. The boundary conditions provided for in this analysis and the longitudinal functions that are used for each are shown in Table I. These longitudinal functions satisfy the kinematic boundary conditions on the ends of the plate and shell.

As a result of the fact that the cross section of the partitioned shell is symmetric about an axis through the center of the shell and perpendicular to the plate, the mode shapes are either symmetric or antisymmetric about this axis. Therefore, no coupling exists between the symmetric and antisymmetric circumferential shell functions. This is also true for the transverse plate functions. This uncoupling allows the equations of motion to be solved separately for the symmetric and antisymmetric modes.

The circumferential functions that are used for the shell are as follows:

TABLE I

KINEMATIC BOUNDARY CONDITIONS AND LONGITUDINAL FUNCTIONS
IN THE ASSUMED DISPLACEMENT SERIES

Boundary Condition				Longitudinal Functions, $\phi_m(x)$
Type		Shell	Plate	
Freely Supported	x = 0:	$v_s = w_s = 0$	$v_p = w_p = 0$	$\phi_m(x) = \sin \frac{m\pi x}{L}$
	x = L:	$v_s = w_s = 0$	$v_p = w_p = 0$	
Clamped-Clamped	x = 0: x = L:	$u_s = v_s = w_s = \frac{\partial w_s}{\partial x} = 0$	$u_p = v_p = w_p = \frac{\partial w_p}{\partial x} = 0$	$\phi_m(x)$ = mth mode function of a clamped-clamped beam.[a]
Clamped-Free	x = 0:	$u_s = v_s = w_s = \frac{\partial w_s}{\partial x} = 0$	$u_p = v_p = w_p = \frac{\partial w_p}{\partial x} = 0$	$\phi_m(x)$ = mth mode function of a clamped-free beam.[a]
	x = L:	None	None	
Free-Free	x = 0: x = L:	None	None	$\phi_0(x) = 1$ $\phi_1(x) = \frac{x}{L} - \frac{1}{2}$ $\phi_m(x)$ = (m-1)th mode function of a free-free beam,[a] ($m \geq 2$).

[a] The beam mode functions are given in Appendix D.

For symmetric modes,

$$\psi_{un} = \cos n\theta$$
$$\psi_{vn} = \sin n\theta \qquad (2.29)$$
$$\psi_{wn} = \cos n\theta.$$

For antisymmetric modes,

$$\psi_{un} = \sin n\theta$$
$$\psi_{vn} = -\cos n\theta \qquad (2.30)$$
$$\psi_{wn} = \sin n\theta.$$

The plate transverse functions are:

For symmetric modes,

$$\xi_{un} = \cos \frac{n\pi y}{2b}$$
$$\xi_{vn} = \sin \frac{n\pi y}{2b} \qquad (2.31)$$
$$\xi_{wn} = \cos \frac{n\pi y}{2b}.$$

For antisymmetric modes,

$$\xi_{un} = \sin \frac{n\pi y}{2b}$$
$$\xi_{vn} = -\cos \frac{n\pi y}{2b} \qquad (2.32)$$
$$\xi_{wn} = \sin \frac{n\pi y}{2b}.$$

Constraint Equations

The displacement compatibility conditions that must be satisfied in this analysis can be classifed as either external or internal to the structure. The external kinematic compatibility conditions, or boundary conditions, at the ends of the structure are satisfied by the displacement functions. These functions also satisfy internal compatibility

separately within the plate and within the shell, since they are single valued, continuous, and differentiable. However, they do not satisfy internal compatibility between the plate and shell. This compatibility will be enforced by writing constraint equations.

The compatibility conditions between the plate and shell take the form of equations which state that the shell displacements and rotations at the joint are equal to those of the plate at the joint. If the displacement components of the shell at the joint (located at $\theta = \theta_o$) are transformed to the plate coordinate system and equated to the plate displacements at the joint, the following equations result (see Appendix E):

$$\begin{aligned} u_s &= u_p \\ v_s \cos\theta_o - w_s \sin\theta_o &= v_p \\ v_s \sin\theta_o + w_s \cos\theta_o &= w_p. \end{aligned} \tag{2.33}$$

The rotations of the plate and shell at each point along the joint must also be compatible. As a result of the fact that Equation (2.33) requires the shell and plate displacements to be the same at every point along the joint, the rotations about an axis perpendicular to the joint line at any point will be the same. Thus constraint equations are unnecessary for the two rotations about axes perpendicular to the joint line. This is shown in Appendix E. The remaining rotation about the joint line must be equal for the plate and shell at the joint, if the joint is rigid.

Equating these rotations results in the following compatibility equation:

$$\frac{1}{r}\frac{\partial w_s}{\partial \theta} - \frac{v_s}{r} = \frac{\partial w_p}{\partial y}.$$

A hinged joint between the plate and shell will allow a relative rotation, so this compatibility equation is omitted for a hinged joint.

Thus the compatibility equations for a rigid joint in terms of the displacements are:

$$\begin{aligned} u_s - u_p &= 0 \\ v_s \cos\theta_o - w_s \sin\theta_o - v_p &= 0 \\ v_s \sin\theta_o + w_s \cos\theta_o - w_p &= 0 \\ \frac{v_s}{r} - \frac{1}{r}\frac{\partial w_s}{\partial \theta} + \frac{\partial w_p}{\partial y} &= 0 \end{aligned} \tag{2.34}$$

For use in the analysis, these compatibility equations must be stated in terms of the generalized coordinates. This is done by substituting the displacement functions into Equation (2.34).

For the first of Equation (2.34), this results in the following:

$$\sum_{m=0}^{m^*} \phi_m(x) \sum_{n=0}^{n^*} [U^s_{mn}\, \psi_{un}(\theta_o) - U^p_{mn}\, \xi_{un}(y_o)] = 0.$$

This can be satisfied by requiring

$$\sum_{n=0}^{n^*} [U^s_{mn}\, \psi_{un}(\theta_o) - U^p_{mn}\, \xi_{un}(y_o)] = 0 \quad (m = 0, 1, \ldots, m^*) \tag{2.35a}$$

The remaining constraint equations are obtained from Equation (2.34) in a similar manner. They are:

$$\sum_{n=0}^{n^*} [V^s_{mn}\, \psi_{vn}(\theta_o) \cos\theta_o - W^s_{mn}\, \psi_{wn}(\theta_o) \sin\theta_o - V^p_{mn}\, \xi_{vn}(y_o)] = 0$$

$$(m = 0, 1, \ldots, m^*) \tag{2.35b}$$

$$\sum_{n=0}^{n^*} [V^s_{mn}\, \psi_{vn}(\theta_o) \sin\theta_o + W^s_{mn}\, \psi_{wn}(\theta_o)\cos\theta_o - W^p_{mn}\, \xi_{wn}(y_o)] = 0$$

$$(m = 0, 1, \ldots, m^*) \quad (2.35c)$$

$$\sum_{n=0}^{n^*} [\frac{1}{r} V^s_{mn}\, \psi_{vn}(\theta_o) - \frac{1}{r} W^s_{mn} \frac{\partial \psi_{wn}}{\partial \theta}(\theta_o) + W^p_{mn} \frac{\partial \xi_{wn}}{\partial y}(y_o)] = 0$$

$$(m = 0, 1, \ldots, m^*) \quad (2.35d)$$

The use of the same longitudinal displacement functions for the plate and shell is necessary to avoid having the longitudinal functions appear in the constraint equations, and thus to allow compatibility to be enforced at every point along the joint. Otherwise, it would be necessary to impose compatibility at only a number of discrete points along the joint, or to satisfy compatibility in an approximate integral sense.

Because of the symmetry of the cross section of the shell, constraint equations need be written only for one joint. The matrix form of the constraint equations is given in Appendix E.

Computer Solution

The computer program that was written to perform the computations in this analysis allows any of the four boundary conditions given in Table I. Orthotropic properties are included. The program can analyze either a plate, or a shell, or a partitioned shell. It permits the use of a different number of terms in each displacement series. Efficient use is made of computer storage by storing only the upper triangular part of symmetric matrices.

The user of the program can specify the operations it is to perform in an analysis by means of a series of data cards containing key words

that instruct the program to perform a certain operation, or series of operations. This allows flexibility in the use of the program. The sequence of steps in a typical problem is shown in Table II.

The two sets of generalized coordinates for the plate and shell are not independent, since they are related by the constraint equations. It is necessary to identify a set of dependent coordinates in order to partition the constraint matrix as in Equation (2.21) to form the transformation matrix of Equation (2.24). The number of dependent coordinates is equal to the rank of the constraint matrix. It is sometimes difficult to determine the rank of the constraint matrix by inspection or to choose which coordinates form a dependent set. An incorrect choice can cause numerical difficulties or erroneous results. To avoid this difficulty, a scheme was implemented to automatically choose a set of independent coordinates. This was done by using a Gauss elimination subroutine with complete pivoting to determine the rank of the constraint matrix. This subroutine, called DMFGR, is described in Reference (23). The rows and columns of the constraint matrix are rearranged in the process, with the independent coordinates placed first. The transformation matrix of Equation (2.24) is automatically generated in the process. The mass and stiffness matrices can then be transformed to independent coordinates by Equation (2.23).

The frequencies and mode shapes are found by solving the eigenvalue problem:

$$[K]\ \{q_1\} = \omega^2\ [M]\ \{q_1\}.$$

This problem is usually solved by putting it into the form:

$$[A]\ \{q_1\} = \omega^2\ \{q_1\} \quad \text{where } [A] = [M]^{-1}\ [K]$$

TABLE II

SEQUENCE OF PROGRAM OPERATIONS FOR
A TYPICAL PROBLEM

Step	Operation
1	Read data for shell, plate, and joint. Read the number of terms to be used in displacement series.
2	Generate constraint matrix.
3	Determine an independent set of generalized coordinates and form transformation matrix.
4	Evaluate longitudinal integrals.
5	Evaluate shell circumferential integrals.
6	Generate shell portions of the mass and stiffness matrices for the unconstrained system.
7	Evaluate plate transverse integrals.
8	Generate plate portions of the mass and stiffness matrices for the unconstrained system.
9	Transform the unconstrained mass and stiffness matrices to yield the constrained system matrices.
10	Solve for eigenvalues and eigenvectors of the system.
11	Transform the eigenvectors from generalized coordinates to actual displacements to determine the mode shapes.
12	Print frequencies, eigenvectors, and mode shapes.
13	Stop.

and solving for the eigenvalues of matrix [A]. This method requires inversion of matrix [M] which is costly in terms of computer time. Also, matrix [A] is not symmetric, therefore requiring more storage space and the use of an eigenvalue routine for nonsymmetric matrices. This procedure is avoided in this analysis by using a method which retains symmetry and eliminates the need for performing any matrix inversions. This method is described in Appendix F.

CHAPTER III

NUMERICAL RESULTS

The method of analysis developed in Chapter II was used for a study of the effects of the joint condition, plate thickness, and plate location on the natural frequencies and modes of partitioned shells. The importance of including the in-plane motion of the plate in the analysis was also investigated. The results of these studies are presented in this chapter.

The frequencies of an isotropic cylindrical shell depend on six geometric and material parameters (Young's modulus, Poisson's ratio, density, radius, length, and thickness) and on the boundary conditions. For a partitioned shell, the properties of the plate, its thickness, its location, and the type of the joint must also be considered. It is necessary to limit the scope of the present investigation because of the large number of variables involved. Thus, the plate is assumed to be of the same material as the shell. Only the freely supported boundary condition is considered. This boundary condition was chosen because the longitudinal displacement functions are exact for this case. Therefore, only one longitudinal term is necessary in the displacement series. The result is a smaller eigenvalue problem than would be the case for other boundary conditions. Also, only the modes with one longitudinal half wave ($\bar{m} = 1$) are considered. These modes will include the fundamental and several of the next lowest modes of the system.

Although no results for shells with interior plates were available for comparison with results of the present method, the computer program was thoroughly tested. The portions of the program involving the shell were checked by comparing the results of several circular cylindrical shell problems with various boundary conditions to those of reference (8), in which Love's shell theory and the Rayleigh-Ritz method were used. The results agreed completely. To test the plate portion of the program, plate problems with several different combinations of boundary conditions were solved. The results were verified by comparing with results given by Leissa (25).

Tests were made to check the convergence of the frequencies as the numbers of terms in the displacement series were increased. The results of one test for a partitioned shell are shown in Table III. Subsequent analyses were generally made with at least eleven circumferential terms in the shell displacement series and seven to nine terms in the plate displacement series. This results in fifty to sixty degrees of freedom. This number of degrees of freedom provides satisfactory accuracy and results in an eigenvalue problem of reasonable size.

Neglecting the In-Plane Motion of the Plate

A study was made to determine the effect of neglecting the in-plane deformation of the plate on the frequencies. It is reasonable to expect that the in-plane deformation of the plate will be small compared to the bending displacements of the shell and plate, at least in the lower modes. Neglecting the in-plane degrees of freedom of the plate results in a smaller eigenvalue problem than if they are included.

TABLE III

CONVERGENCE OF FREQUENCIES FOR A PARTITIONED SHELL[a)]

Frequencies (hz.) of Several Symmetric Modes				
$\bar{N}_s$[b)]	4	6	11	13
$\bar{N}_p$[c)]	5	7	9	14
	3.21	3.07	3.00	2.95
	12.00	11.94	11.90	11.87
	14.44	14.33	14.23	14.14
	16.42	15.62	15.30	15.14
	22.94	22.63	22.51	22.44

a) The parameters of the shell are: $R = 10$ in., $E = 10^7$ psi, $\nu = 0.3$, $\rho = 0.1$ lb-sec^2/in.^{3}, $t_s/R = 0.02$, $L/\bar{m}R = 2$, $t_p/t_s = 1$, $\theta_o = 90°$, rigid joint.

b) $\bar{N}_s$ = number of circumferential shell terms in the displacement series.

c) $\bar{N}_p$ = number of transverse plate terms in the displacement series.

When the plate is at the center of the shell, its in-plane deformation and bending are uncoupled. Either in-plane deformation or bending alone occurs in each mode. This is a result of the symmetry of the structure about the middle plane of the plate. Thus, since some modes exhibit only bending of the plate, neglecting the in-plane degrees of freedom has no effect on the frequencies of these modes. This fact is shown by the frequencies presented in Table IV. The errors in the other frequencies in Table IV are small.

When the plate is not at the center of the shell, the errors incurred by neglecting the in-plane degrees of freedom of the plate are larger, as shown in Table V. The magnitude of the error depends on the amount of in-plane motion of the plate. It was found that these errors could be reduced by including only a few in-plane degrees of freedom. The results of an analysis which included eight terms in the displacement series for w_p and only three terms each for u_p and v_p are also shown in Table V. This procedure yielded excellent results and also reduced the size of the eigenvalue problem. The procedure of using only one-third to one-half as many terms in the displacement series for u_p and v_p as in the series for w_p was adopted for most of the subsequent analyses.

The Effects of the Joint Condition on the Frequencies and Mode Shapes

The results of analyses of partitioned shells with rigid and hinged joints between the shell and the interior plate were compared to determine how the frequencies and mode shapes differed for the two joint conditions.

TABLE IV

THE EFFECT OF NEGLECTING THE PLATE IN-PLANE DEGREES OF FREEDOM ON THE FREQUENCIES OF A PARTITIONED SHELL[a] WITH THE PLATE AT THE CENTER

Frequencies (hz.) of Symmetric Modes		
Including In-Plane Degrees of Freedom	Neglecting In-Plane Degrees of Freedom	Percent Difference
3.07	3.07	0.0
11.94	11.94	0.0
13.94	13.99	0.36
14.33	14.33	0.0
15.62	15.62	0.0
20.95	21.09	0.67
22.63	22.63	0.0
26.79	27.07	1.0

[a] The material and geometric parameters of the shell are given in Table III.

TABLE V

FREQUENCIES OF A PARTITIONED SHELL[a] WITHOUT THE PLATE IN-PLANE DEGREES OF FREEDOM AND WITH FEWER IN-PLANE THAN BENDING DEGREES OF FREEDOM

Frequencies (hz.) of Antisymmetric Modes				
1[b] All u_p, v_p Terms Included	2[b] All u_p, v_p Terms Neglected	3[c] Fewer u_p, v_p Than w_p Terms	Percent Difference 1 and 2	Percent Difference 1 and 3
4.75	4.78	4.75	0.6	0.0
6.81	6.86	6.81	0.7	0.0
8.00	8.39	8.01	4.9	0.1
11.09	11.42	11.11	3.0	0.2
14.01	14.07	14.15	0.4	1.0
14.66	15.30	14.66	4.4	0.0
19.49	20.64	19.51	5.9	0.1
21.13	25.01	21.15	18.4	0.1

a) The parameters of the shell are given in Table III.

b) $\bar{N}_s = 13$, $\bar{N}_p = 8$.

c) For u_s and v_s, $\bar{N}_s = 11$; for w_s, $\bar{N}_s = 13$. For u_p and v_p, $\bar{N}_p = 3$; for w_p, $\bar{N}_p = 8$.

The circumferential mode shapes of a partitioned shell with a hinged joint are shown in Figures 2 and 3. These figures show a cross section of the partitioned shell with its exaggerated deformed shape superimposed. The relative amplitudes shown in these diagrams are the same at any cross section. A typical longitudinal mode shape for a partitioned shell is shown in Figure 4. The longitudinal mode shapes for all cases considered in this study are half sine waves.

The mode shapes of an unpartitioned circular cylindrical shell are described by the number of longitudinal half waves and the number of circumferential full waves. However, for the partitioned shell, it is often difficult to assign a circumferential wave number to the mode shape, except for the first few modes. This is especially true for the case of a rigid joint between the plate and shell. The wave numbers do not completely describe the mode shapes for a partitioned shell, so they are not as useful as they are for the unpartitioned shell. However, when possible, wave numbers for the plate and shell will be given in the results that follow, to help identify the frequencies with their corresponding modes.

The mode shapes of Figures 2 and 3 indicate that in many modes the shell exhibits bending in the circumferential direction, but there is no bending of the plate in the transverse (y) direction. The remaining modes involve bending of the plate in the transverse direction, but negligible motion of the shell.

The mode having the lowest frequency exhibits bending motion of the plate, but negligible deformation of the shell. Therefore, the plate is essentially simply supported on all edges. Thus, the fundamental frequency of the structure is very close to that of the plate alone with

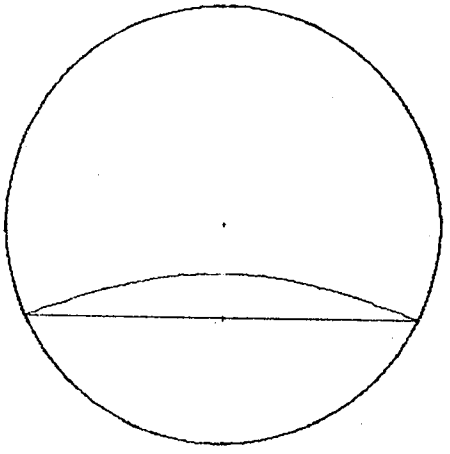

Ω = 0.0196

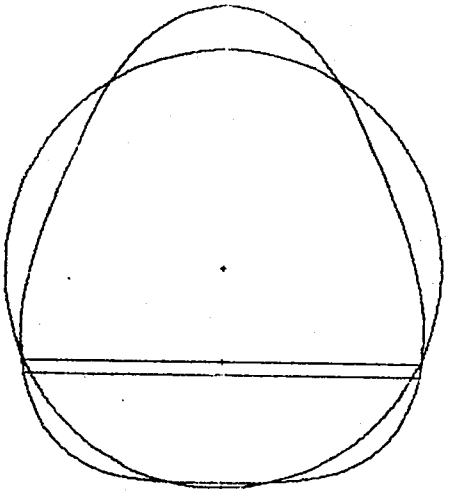

Ω = 0.068

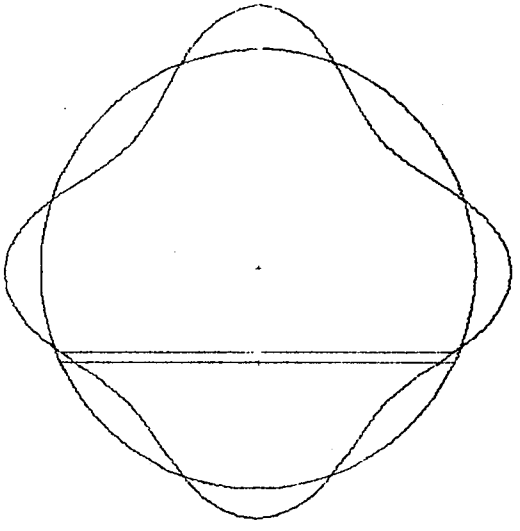

Ω = 0.0871

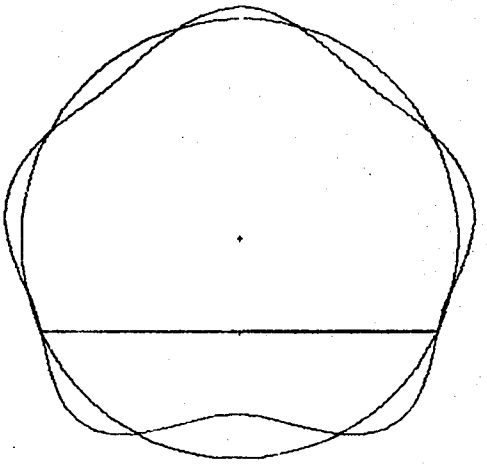

Ω = 0.115

Figure 2. Symmetric Mode Shapes of a Shell With a Hinged Joint (θ_o = 115°, $t_p = t_s$)

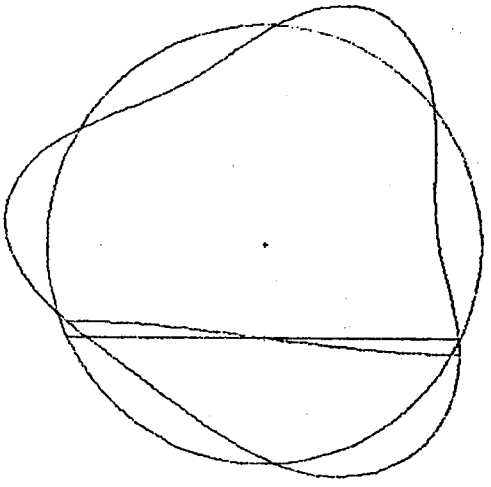

$\Omega = 0.0614$

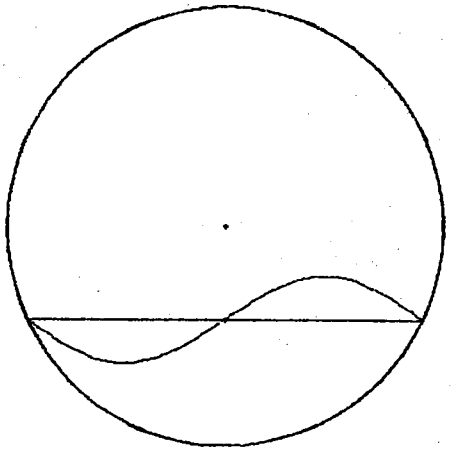

$\Omega = 0.0716$

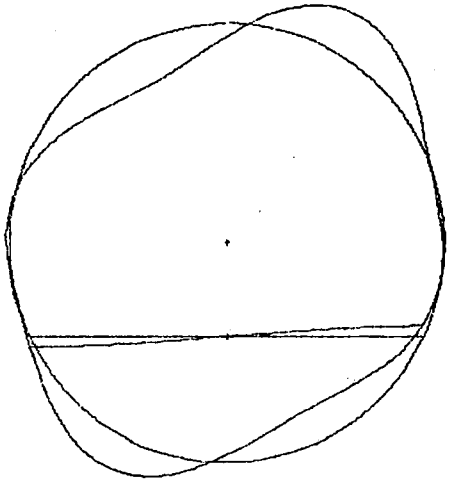

$\Omega = 0.0830$

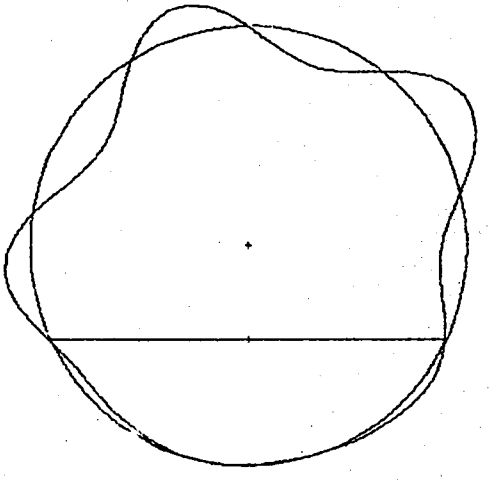

$\Omega = 0.127$

Figure 3. Antisymmetric Mode Shapes of a Shell With a Hinged Joint ($\theta_o = 115°$, $t_p = t_s$)

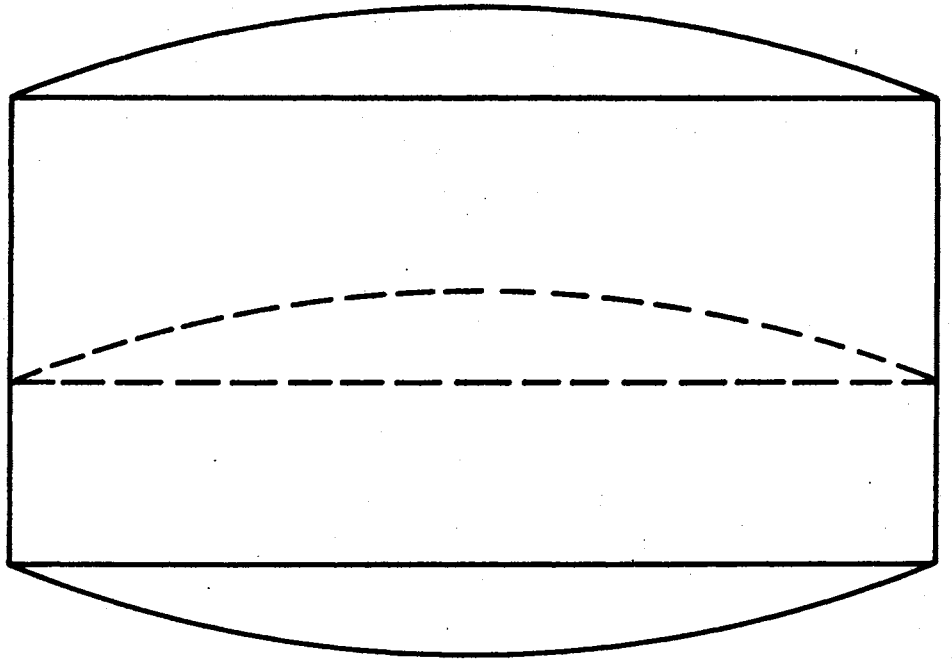

Figure 4. A Typical Longitudinal Mode Shape ($\bar{m} = 1$)

simply supported boundary conditions. Some higher modes also have these characteristics.

In the lowest mode involving appreciable shell motion, the shell has three circumferential waves. This is the same number of waves associated with the lowest frequency of the unpartitioned shell.

The mode shapes and frequencies for a partitioned shell with a rigid joint are shown in Figures 5 and 6. The circumferential bending of the shell and the transverse bending of the plate are coupled in this case. However, some modes exist in which the amplitude of either the shell or the plate is predominant. For example, the lowest mode exhibits primarily bending deformation of the plate. Thus, the frequency of this mode will be between those of a simply supported plate and a plate which is clamped on opposite edges, when the shell does not have a significant amplitude.

It is seen from a comparison of Figures 2 and 3 with Figures 5 and 6 that for the lower modes, the shapes of the shell are almost the same for the rigid and hinged joints. These figures are for the case of equal plate and shell thicknesses. This indicates that for this case, the major effect of the plate on the mode shapes of the shell is its in-plane restraint, which is present for both joint conditions.

A comparison of the frequencies of partitioned shells having rigid and hinged joints is shown in Table VI. It may be observed that some frequencies are almost the same for the rigid and hinged joint conditions. The mode shapes indicate that these frequencies correspond to modes in which the bending of the plate is small. Thus, the in-plane restraint of the plate on the shell is the major effect. This in-plane

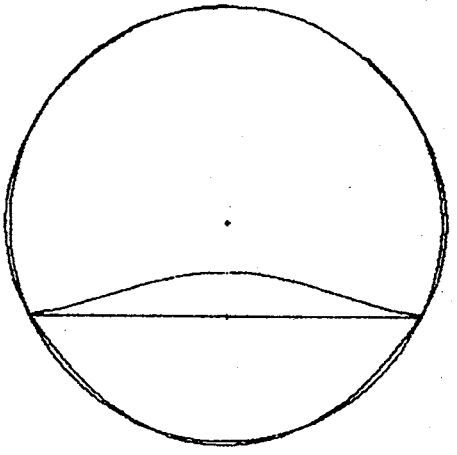

$\Omega = 0.0367$

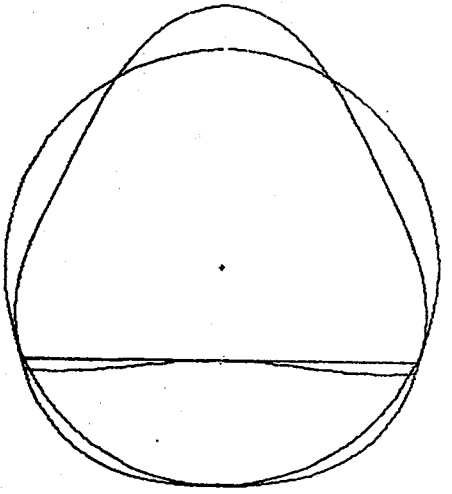

$\Omega = 0.0693$

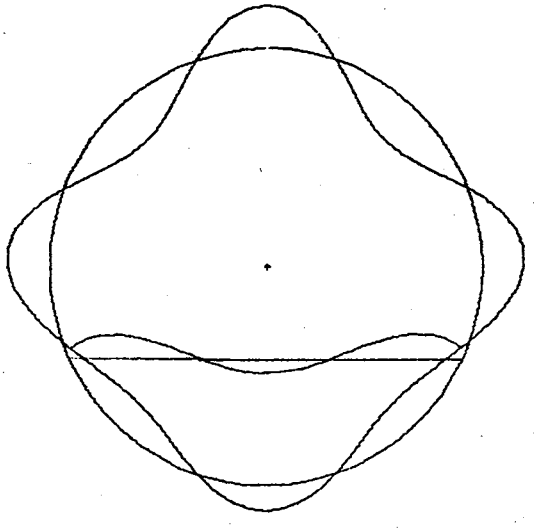

$\Omega = 0.0939$

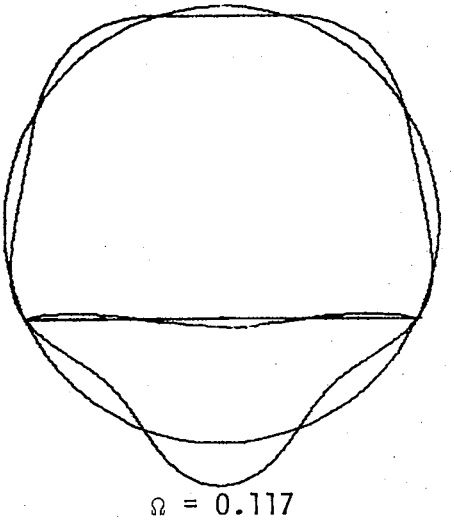

$\Omega = 0.117$

Figure 5. Symmetric Mode Shapes of a Shell With a Rigid Joint ($\theta_o = 115°$, $t_p = t_s$)

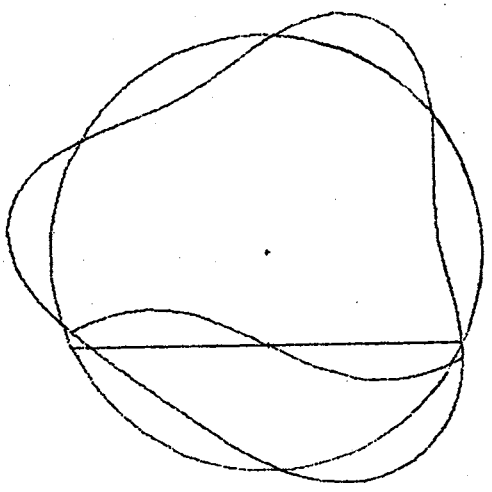

$\Omega = 0.0625$

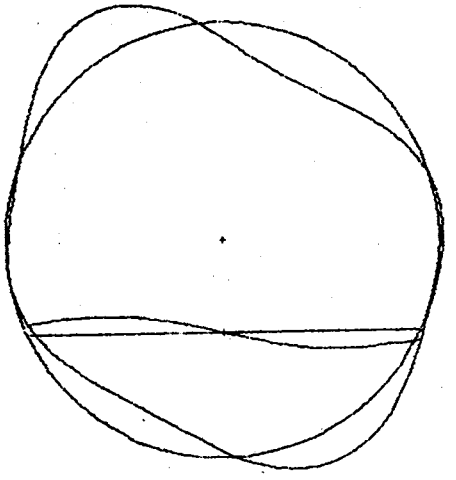

$\Omega = 0.0828$

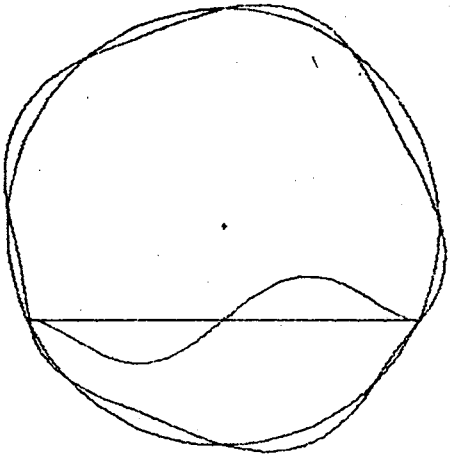

$\Omega = 0.103$

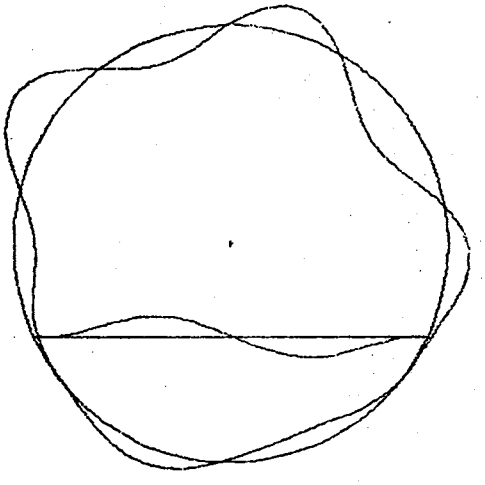

$\Omega = 0.133$

Figure 6. Antisymmetric Mode Shapes of a Shell With a Rigid Joint ($\theta_o = 115°$, $t_p = t_s$)

TABLE VI

COMPARISON OF THE FREQUENCIES OF A PARTITIONED SHELL[a] WITH RIGID AND HINGED JOINTS

Symmetric Modes						Antisymmetric Modes					
Hinged Joint			Rigid Joint			Hinged Joint			Rigid Joint		
$\bar{n}_s$ [b]	$\bar{n}_p$ [c]	Ω [d]	$\bar{n}_s$	$\bar{n}_p$	Ω	$\bar{n}_s$	$\bar{n}_p$	Ω	$\bar{n}_s$	$\bar{n}_p$	Ω
-	1	.0196	3	1	.0367	3	0	.0614	3	2	.0625
3	0	.0678	3	3	.0693	-	2	.0717	2	2	.0828
4	0	.0871	4	3	.0939	2	0	.0830	5	2	.103
5	0	.115	5	3	.117	5	0	.127			.133
	3	.158			.167			.156			.163
	0	.167			.219			.203			.210

[a] The parameters of the shell are: $R = 10$ in., $\nu = 0.3$, $t_s/R = 0.02$, $L/\bar{m}R = 5$, $t_p/t_s = 1$, $\theta_o = 115°$.

[b] Number of circumferential waves for shell. A dash indicates negligible amplitude.

[c] Number of half waves for the plate in the transverse (y) direction.

[d] Nondimensional frequency.

restraint is the same for both joint conditions, so the frequencies are approximately the same.

Each of the frequencies in Table VI is higher for the shell with the rigid joint than for the case of the hinged joint. This is a result of the greater stiffness of the structure due to the rigid joint. This effect is largest in the modes exhibiting mainly plate bending.

The Effects of Varying the Thickness of the Plate on the Modes and Frequencies

A series of problems was analyzed to study the effect of varying the plate thickness on the frequencies and mode shapes of the system.

The frequencies of a partitioned shell with a hinged plate are shown in Table VII for several values of the plate to shell thickness ratio, with the thickness of the shell remaining constant. As was described before, some modes of the partitioned shell with a hinged joint involve only bending of the plate. For these modes the structure has a frequency equal to that of the plate alone with simply supported edges. Therefore, the frequencies of these modes should vary with the plate thickness in the same manner as those of a simply supported plate, i.e., linearly with thickness. The fundamental frequency, which is plotted in Figure 7 as a function of the thickness ratio, exhibits this behavior, as do some of the higher frequencies in Table VII. Other modes involve primarily motion of the shell and only slight longitudinal bending of the plate. The frequencies of these modes are hardly affected by a change in the plate thickness. This is shown in Figure 7. The slight decrease in frequency as the thickness ratio increases indicates that the greater inertia of the thicker plate has more effect on the

TABLE VII

THE EFFECT OF THE PLATE THICKNESS ON THE FREQUENCIES OF A PARTITIONED SHELL[a] WITH A HINGED JOINT

Shell Only		t_p/t_s = .25			t_p/t_s = .5			t_p/t_s = 1			t_p/t_s = 2			t_p/t_s = 3		
$\bar{n}_s$	Ω	$\bar{n}_s$[b]	$\bar{n}_p$[c]	Ω[d]	$\bar{n}_s$	$\bar{n}_p$	Ω	$\bar{n}_s$	$\bar{n}_p$	Ω	$\bar{n}_s$	$\bar{n}_p$	Ω	$\bar{n}_s$	$\bar{n}_p$	Ω
3	.0595	-	1	.0049	-	1	.0098	-	1	.0196	-	1	.0392	-	1	.0588
2	.0778	-	3	.0395	3	0	.0690	3	0	.0678	3	0	.0651	3	0	.0626
4	.0887	3	0	.0696	-	3	.0792	4	0	.0871	4	0	.0857	4	0	.0848
5	.139	4	0	.0883	4	0	.0879	5	0	.115	5	0	.116	5	0	.116
6	.220	-	5	.109	5	0	.115	6	3	.158	6	0	.158	6	0	.151
7	.277	5	0	.114	6	0	.175		0	.167		0	.183		0	.183

[a] The parameters of the structure are given in Table VI.

[b] Number of circumferential waves for the shell. A dash indicates negligible amplitude.

[c] Number of half waves for the plate in the y direction.

[d] Nondimensional frequency for symmetric modes.

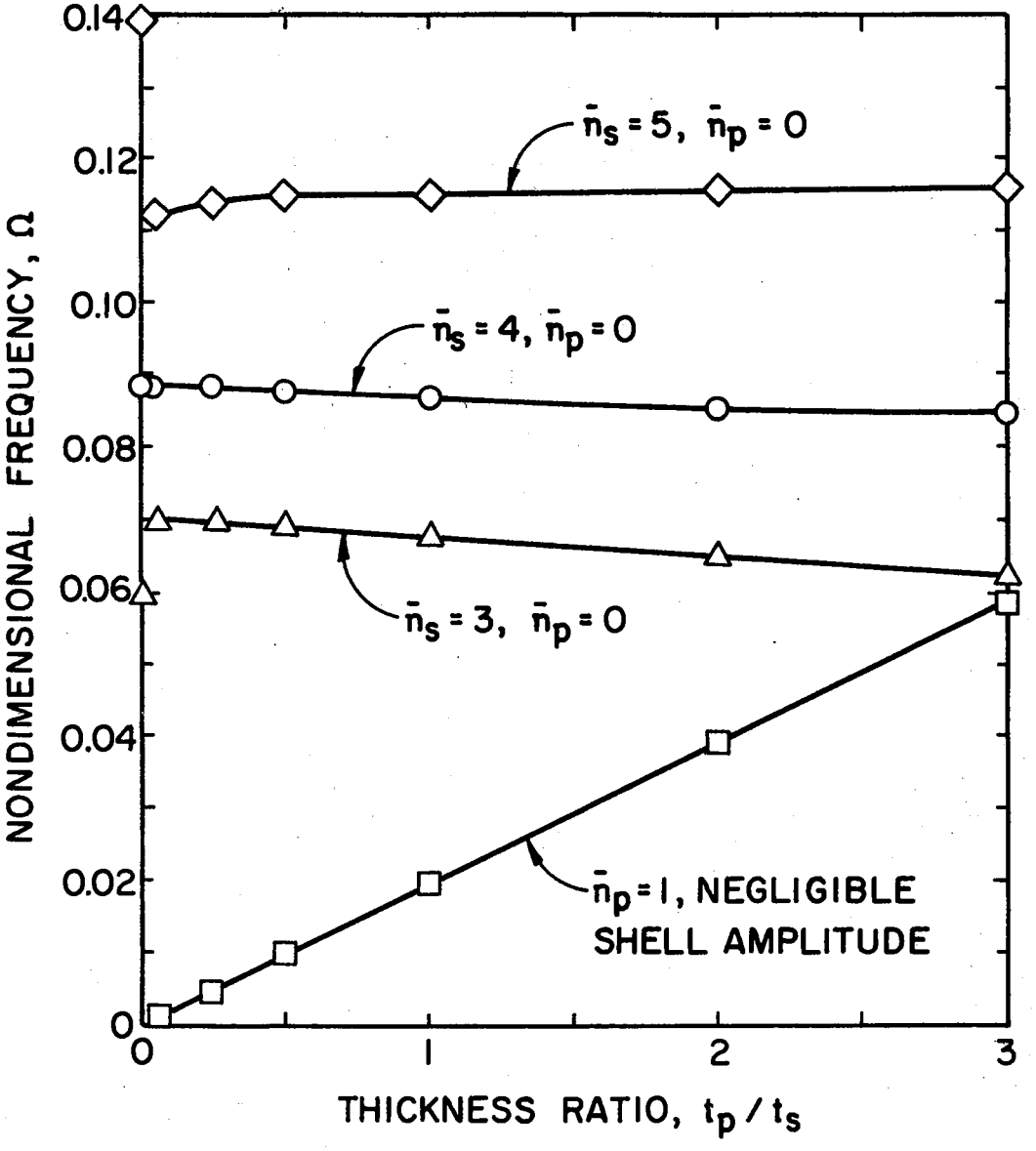

Figure 7. The Effect of the Plate Thickness on the Frequencies of a Shell With a Hinged Joint (θ_o = 115°, Symmetric Modes)

frequencies than does the increase in stiffness. This slight decrease is not observed for the frequency of the mode involving five circumferential shell waves. The mode shape indicates that there is negligible plate motion in this case. Thus, the inertia effect is not observed in this mode.

The lowest value of the thickness ratio plotted in Figure 7 is 0.05. At this small value the frequencies of some modes do not yet approach those of the unpartitioned shell. The transition must occur for even smaller thickness. Thus, the in-plane restraint provided by even a very thin plate is sufficient to alter the frequency and mode shape of the unpartitioned shell. Also, as the plate thickness becomes very small, the frequencies of those modes involving only motion of the plate become small, and a greater number of these modes have frequencies less than the lowest mode involving appreciable shell motion.

The order of the modes in the frequency spectrum will change when the thickness of the plate is changed, because the frequencies of some modes change with thickness while others show little change. This effect is shown in Table VII, in which the modes are identified by their wave numbers. This behavior can also be noted in Figure 7. By extrapolating the curves, it is seen that if the thickness ratio is larger than about 3.2, the mode which exhibits one-half wave in the plate and negligible shell motion will no longer have the lowest frequency.

The frequencies of a partitioned shell with a rigid joint are presented in Tables VIII and IX for several values of the thickness ratio. Circumferential mode shapes for different plate thicknesses are shown in Figures 8, 9, and 10.

TABLE VIII

THE EFFECT OF THE PLATE THICKNESS ON THE FREQUENCIES OF SYMMETRIC MODES OF A PARTITIONED SHELL[a] WITH A RIGID JOINT

Shell Only		t_p/t_s = .25			t_p/t_s = .5			t_p/t_s = 1			t_p/t_s = 2			t_p/t_s = 3		
$\bar{n}_s$	Ω	$\bar{n}_s$[b]	$\bar{n}_p$[c]	Ω[d]	$\bar{n}_s$	$\bar{n}_p$	Ω	$\bar{n}_s$	$\bar{n}_p$	Ω	$\bar{n}_s$	$\bar{n}_p$	Ω	$\bar{n}_s$	$\bar{n}_p$	Ω
3	.0595	-	1	.0108	-	1	.0213	3	1	.0367	3	1	.0492	3	1	.0605
2	.0778	-	3	.0578	3	3	.0692	3	3	.0693	3	3	.0695	3	1	.0700
4	.0887	3	5	.0696	4	3	.0872	4	3	.0939	4	3	.104	4	1	.104
5	.139	4	5	.0885	5	3	.113	5	3	.117	5	3	.128			.133
6	.220			.114			.119			.167			.157			.151
7	.227			.144			.175			.219			.197			.213

[a] The parameters of the shell are given in Table VI.

[b] Number of circumferential waves for the shell. A dash indicates negligible amplitude.

[c] Number of half waves for the plate in the y direction.

[d] Nondimensional frequency.

TABLE IX

THE EFFECT OF THE PLATE THICKNESS ON THE FREQUENCIES OF THE ANTISYMMETRIC MODES OF A PARTITIONED SHELL[a] WITH A RIGID JOINT

t_p/t_s = .25			t_p/t_s = .5			t_p/t_s = 1			t_p/t_s = 2			t_p/t_s = 3		
$\bar{n}_s$[b]	$\bar{n}_p$[c]	Ω[d]	$\bar{n}_s$	$\bar{n}_p$	Ω	$\bar{n}_s$	$\bar{n}_p$	Ω	$\bar{n}_s$	$\bar{n}_p$	Ω	$\bar{n}_s$	$\bar{n}_p$	Ω
3	2	.0295	3	2	.0560	3	2	.0625	3	2	.0703	3	2	.0735
3	4	.0618	3	4	.0651	2	2	.0828	2	2	.0843	2	2	.0856
2	4	.0816	2	4	.0824	5	2	.103	4	2	.131	4	2	.138
		.0954			.125	4	2	.133			.153			.169
		.121			.153			.163			.182			.211

[a] The parameters of the shell are given in Table VI.

[b] Number of circumferential waves for the shell.

[c] Number of half waves for the plate in the y direction.

[d] Nondimensional frequency.

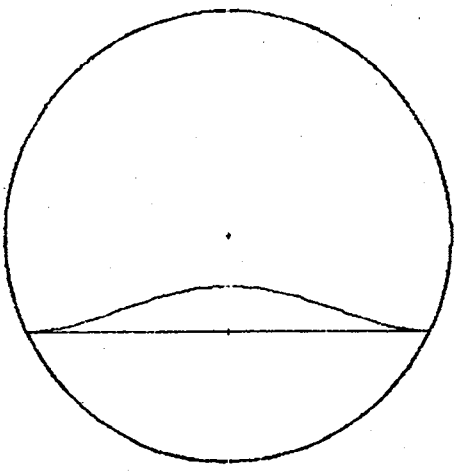

$t_p/t_s = .5$

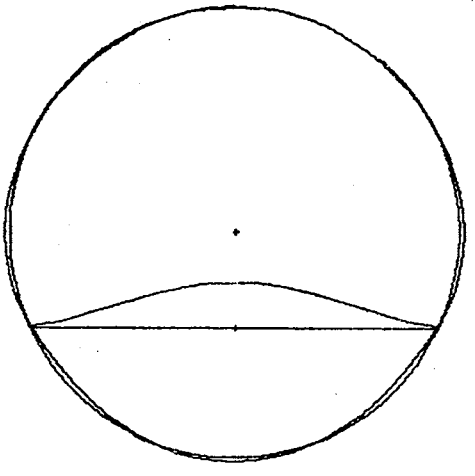

$t_p/t_s = 1$

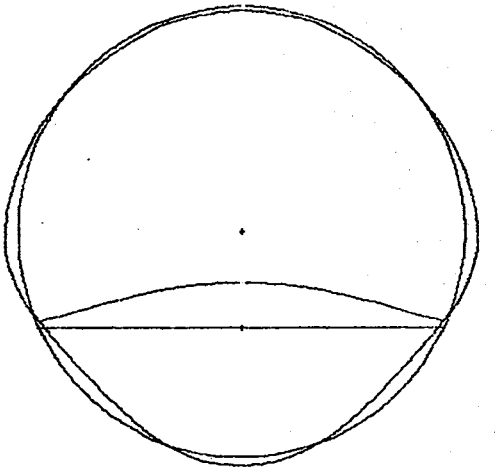

$t_p/t_s = 2$

Figure 8. Fundamental Mode for Various Plate Thicknesses ($\theta_o = 115°$, Rigid Joint)

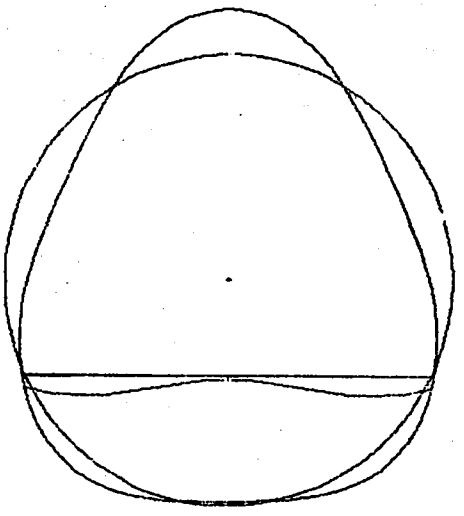

$t_p/t_s = .5$

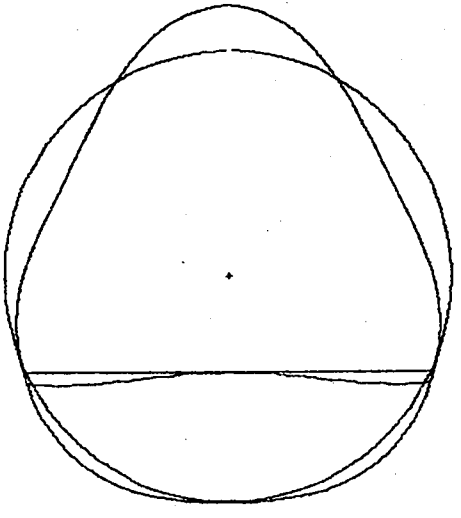

$t_p/t_s = 1$

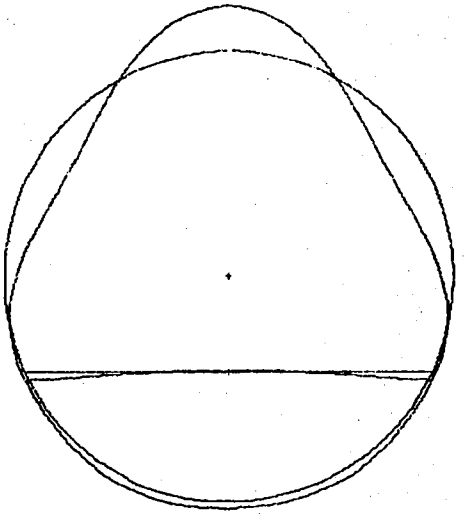

$t_p/t_s = 2$

Figure 9. Second Symmetric Mode for Various Plate Thicknesses (θ_o = 115°, Rigid Joint)

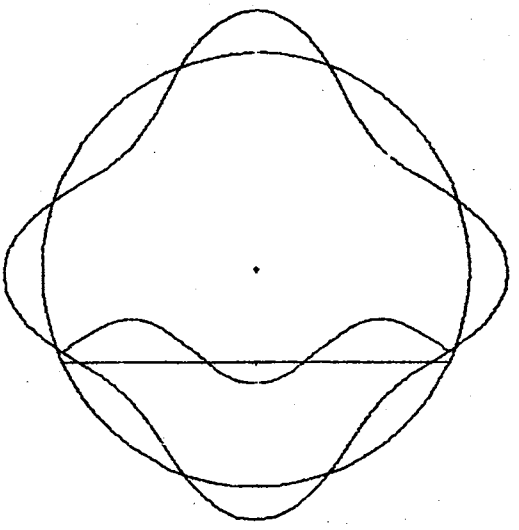

$t_p/t_s = .5$

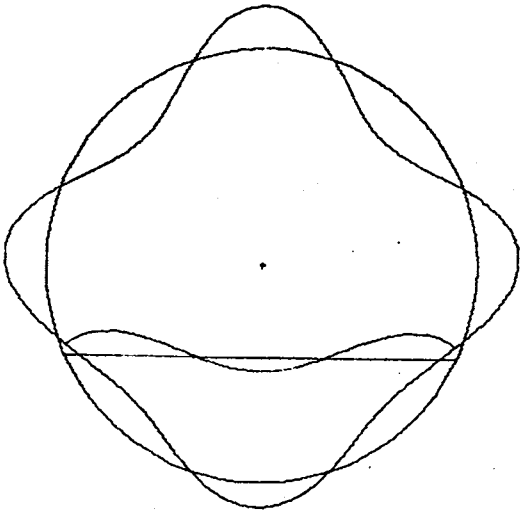

$t_p/t_s = 1$

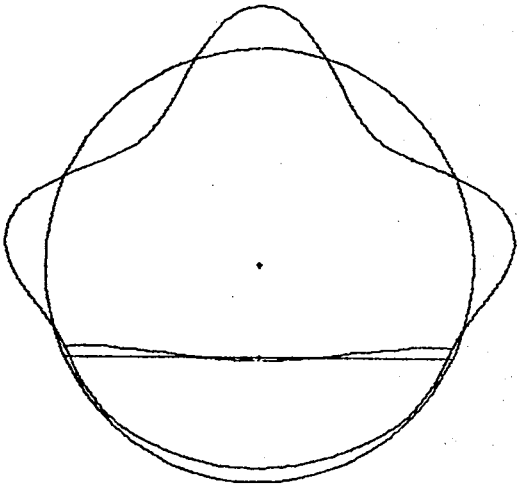

$t_p/t_s = 2$

Figure 10. Third Symmetric Mode for Various Plate Thicknesses ($\theta_o = 115°$, Rigid Joint)

As shown in Figure 8, the fundamental mode of the system, for the case of a rigid joint,involves predominantly motion of the plate. The frequency of this mode is plotted in Figure 11 as a function of the thickness ratio. This frequency increases significantly as the plate thickness increases.

The frequencies of other modes change very little with the thickness ratio (Figure 11). These are modes in which the amplitude of the shell is large compared to the amplitude of the plate. Thus, because the participation of the plate is small, the frequency of the system changes only slightly as the thickness of the plate is increased.

The frequencies of some modes show a mixed behavior (Figure 11) as the thickness of the plate increases. At small thicknesses, the motion of the plate is predominant and the frequency increases with the plate thickness. At larger thicknesses, the curves tend to flatten out. It is seen from the mode shape plots that as the plate thickness increases, the amplitude of its vibration decreases. Thus, as the plate participates less in the motion, the frequency becomes less sensitive to changes in the plate thickness.

As was the case for the hinged joint, the fact that the frequencies of some modes depend more strongly on the thickness ratio than do others may change the order of the mode shapes in the frequency spectrum. Also, from Tables VIII and IX, it can be seen that the frequencies tend to become more closely spaced as the thickness ratio decreases.

Figures 12 and 13 show the mode shapes of a partitioned shell with the plate located farther from the center of the shell (θ_o = 135°) than in the case discussed above (θ_o = 115°). This problem was considered in

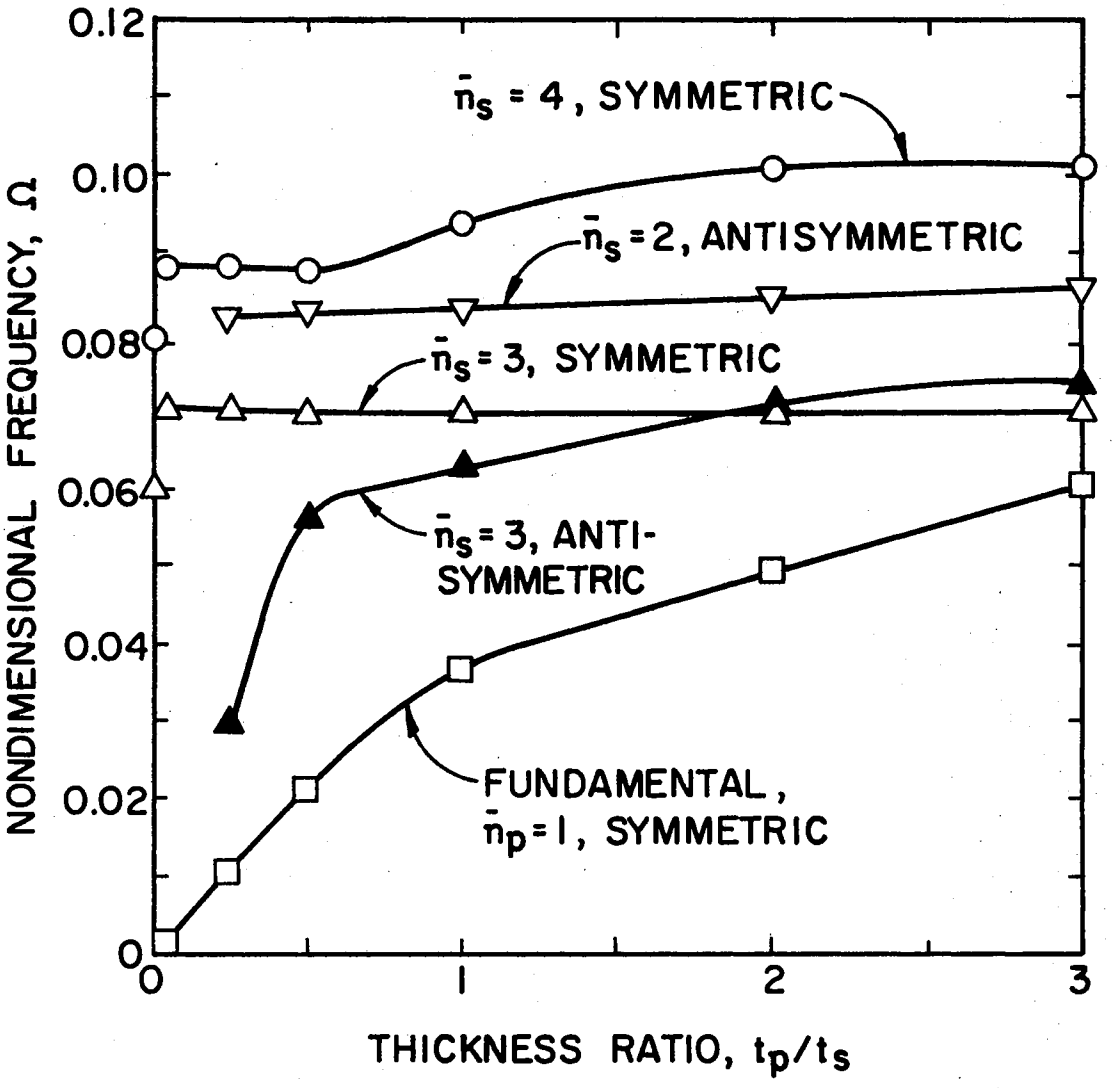

Figure 11. The Effect of the Plate Thickness on the Frequencies of a Shell With a Rigid Joint (θ_o = 115°)

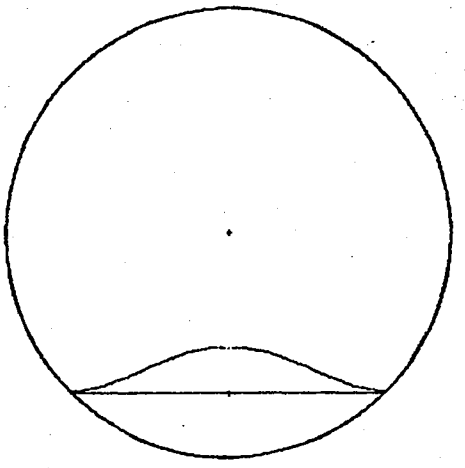

$t_p/t_s = .5$

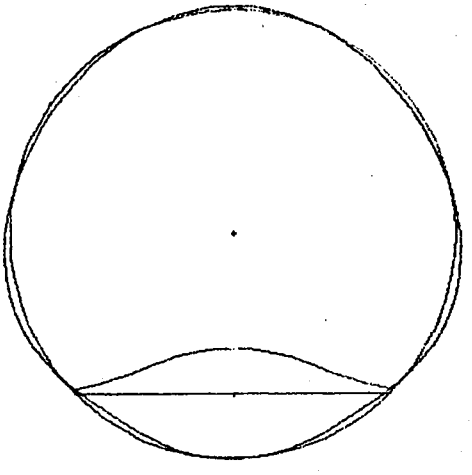

$t_p/t_s = 1$

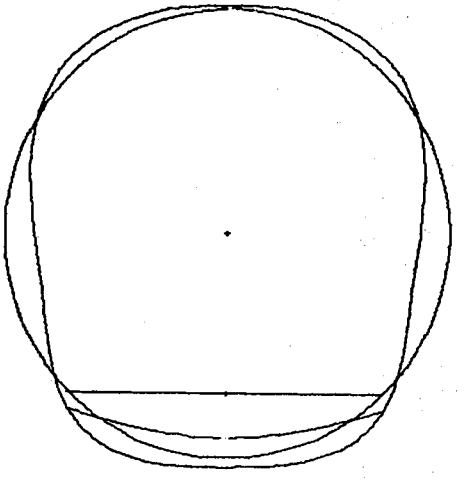

$t_p/t_s = 2$

Figure 12. Fundamental Mode for Various Plate Thicknesses ($\theta_o = 135°$, Rigid Joint)

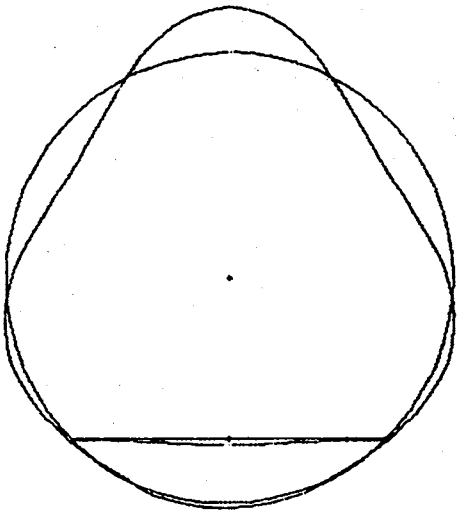

$t_p/t_s = .5$

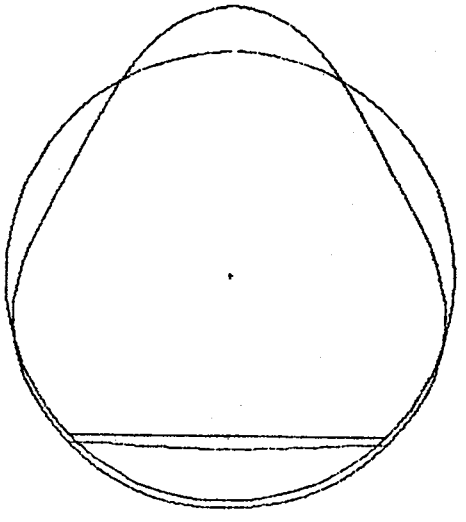

$t_p/t_s = 1$

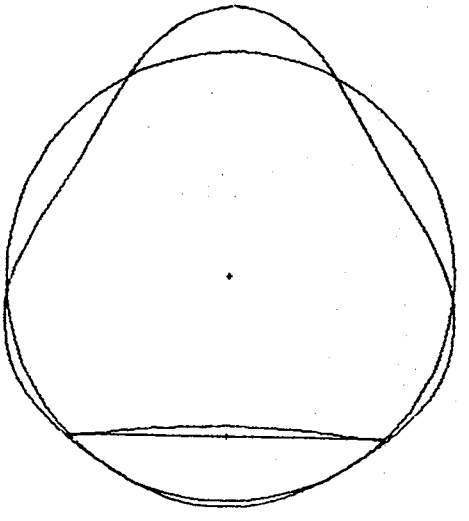

$t_p/t_s = 2$

Figure 13. Second Symmetric Mode for Various Plate Thicknesses ($\theta_o = 135°$, Rigid Joint)

less detail, but the same trends were noted. However, in this case, the amplitude of the plate with respect to the shell was generally smaller.

The Effects of the Location of the Plate on the Modes and Frequencies

The frequencies of a partitioned shell are presented in Tables X and XI for several locations of the plate. The location of the plate is indicated by the value of the θ-coordinate at which the joint is located, θ_o. Figures 14, 15, 16, and 17 show the circumferential mode shapes for several locations of the plate.

The in-plane and bending deformations of the plate are uncoupled when the plate is located at the center of the shell. Thus, the in-plane and bending deformations do not occur in the same mode. In this case, the frequencies of modes that do not involve plate bending are the same for the hinged and rigid joint conditions.

From the mode shapes of Figures 14 to 17, it is seen that the plate tends to bend in fewer waves the farther it is located from the center. The modes usually show the same number of circumferential waves in the shell as the location of the plate changes. However, the character of the modes may change when the plate is located far from the center. For example, it is observed from the wave numbers of Table XI that when $\theta_o = 150°$, the mode having four shell waves is missing from the lower modes, and that a mode having two circumferential waves appears. Also, when there is a rigid joint and the plate is located at large values of θ_o, the bending restraint of the plate suppresses the bending deformation of the shell in the region of the joint. This is shown by the modes of Figures 16 and 17 for $\theta_o = 135°$.

TABLE X

FREQUENCIES OF A PARTITIONED SHELL[a] WITH A HINGED JOINT
FOR SEVERAL LOCATIONS OF THE PLATE

$\theta_o = 90°$			$\theta_o = 105°$			$\theta_o = 115°$			$\theta_o = 135°$			$\theta_o = 150°$		
$\bar{n}_s$[b]	$\bar{n}_p$[c]	Ω[d]	$\bar{n}_s$	$\bar{n}_p$	Ω	$\bar{n}_s$	$\bar{n}_p$	Ω	$\bar{n}_s$	$\bar{n}_p$	Ω	$\bar{n}_s$	n_p	Ω
-	1	.0165	-	1	.0175	-	1	.0196	-	1	.0308	-	1	.0593
3	0	.0576	3	0	.0628	3	0	.0678	3	0	.0706	3	0	.0653
4	0	.0863	4	0	.0870	4	0	.0871	4	0	.0749	2	0	.0752
-	3	.131	5	0	.117	5	0	.115	5	0	.129	5	0	.108
5	0	.136	-	3	.140			.158			.178			.173

[a] The parameters of the shell are given in Table VI.

[b] Number of circumferential waves for the shell. A dash indicates negligible amplitude.

[c] Number of half waves for the plate in the y direction.

[d] Nondimensional frequency of the symmetric modes.

TABLE XI

FREQUENCIES OF A PARTITIONED SHELL[a] WITH A RIGID JOINT FOR SEVERAL LOCATIONS OF THE PLATE

$\theta_o = 90°$			$\theta_o = 105°$			$\theta_o = 115°$			$\theta_o = 135°$			$\theta_o = 150°$		
$\bar{n}_s$[b]	$\bar{n}_p$[c]	Ω[d]	$\bar{n}_s$	$\bar{n}_p$	Ω	$\bar{n}_s$	$\bar{n}_p$	Ω	$\bar{n}_s$	$\bar{n}_p$	Ω	$\bar{n}_s$	$\bar{n}_p$	Ω
-	1	.0296	-	1	.0318	-	1	.0367	-	1	.0572	3	1	.0653
3	3	.0630	3	3	.0667	3	3	.0693	3	1	.0709	2	1	.0752
4	0	.0863	4	3	.0902	4	3	.0939	4	1	.0795	5	1	.104
5	3	.135	5	3	.118	5	3	.117	5	3	.133	6	1	.127
		.164			.166			.167			.178			.178

[a] The parameters of the shell are given in Table VI.

[b] Number of circumferential waves for the shell. A dash indicates negligible amplitude.

[c] Number of half waves for the plate in the y direction.

[d] Nondimensional frequency of the symmetric modes.

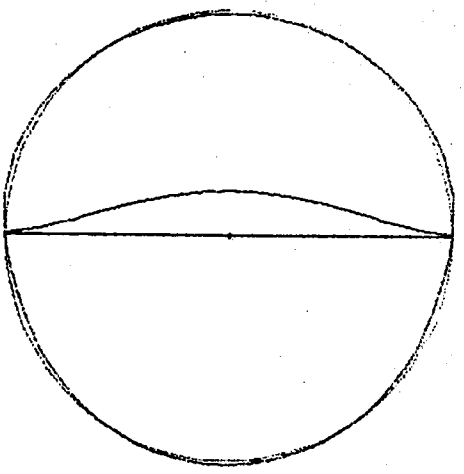

$\theta_o = 90°$

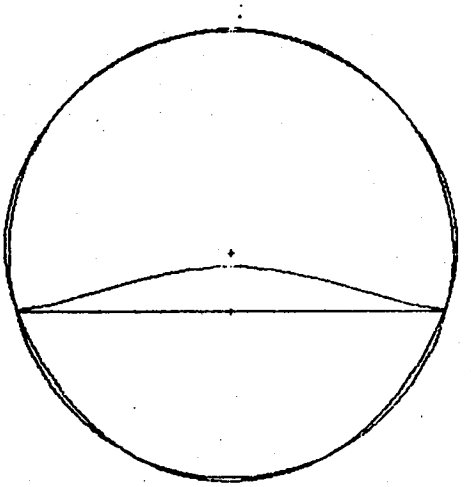

$\theta_o = 105°$

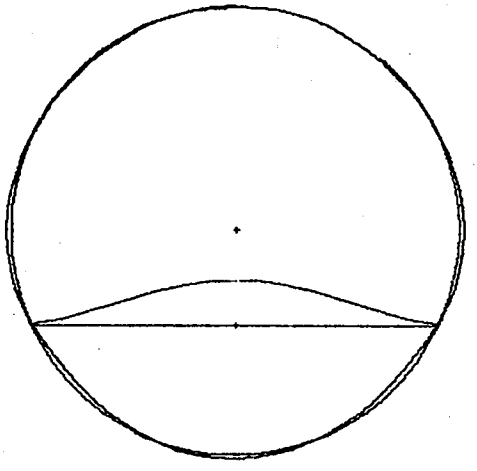

$\theta_o = 115°$

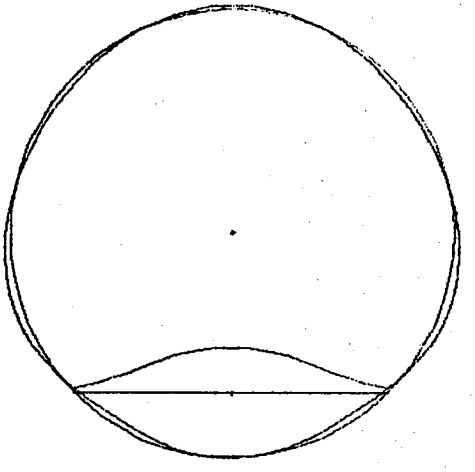

$\theta_o = 135°$

Figure 14. Fundamental Mode for Various Plate Locations (Rigid Joint, $t_p = t_s$)

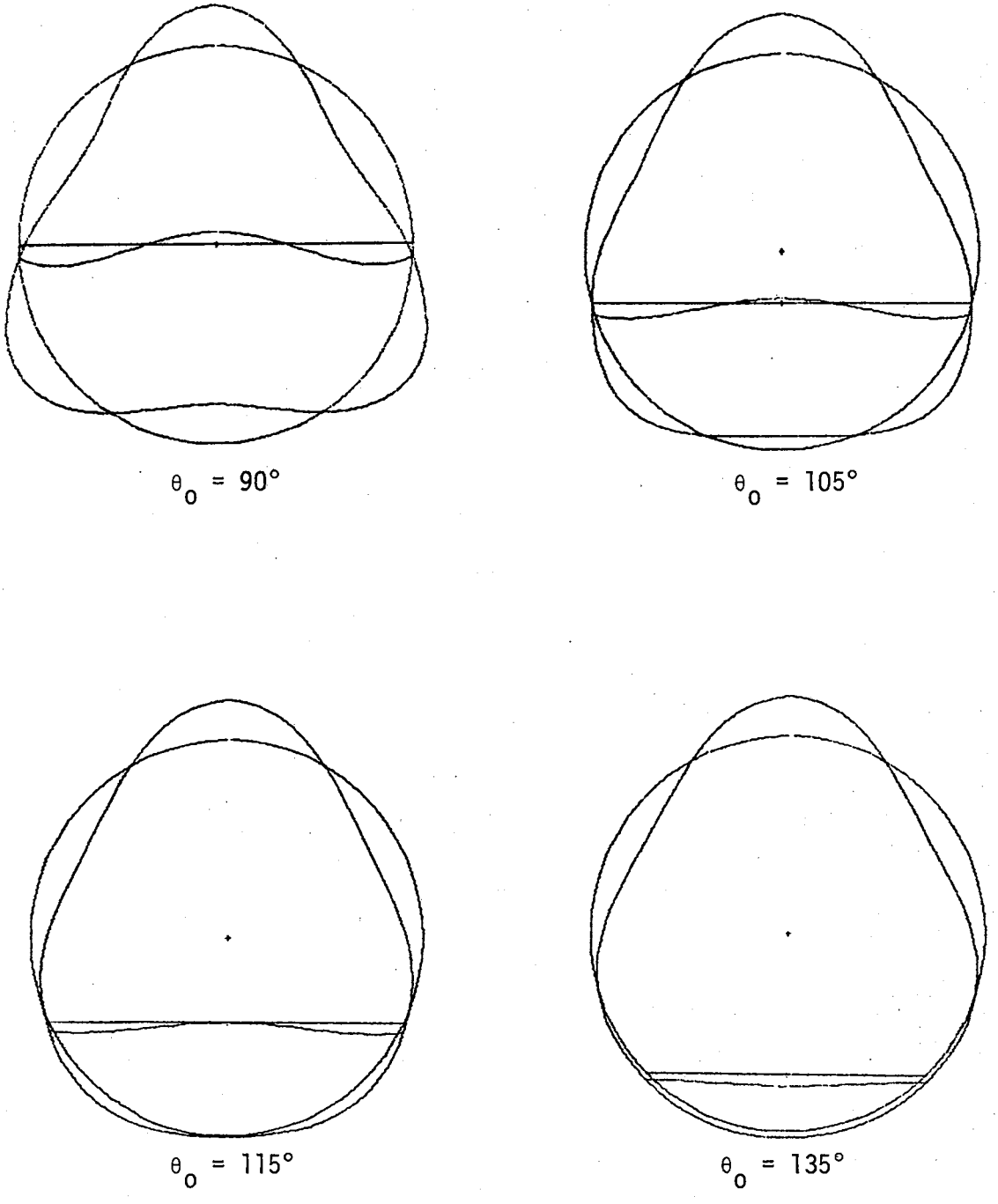

Figure 15. Second Symmetric Mode for Various Plate Locations (Rigid Joint, $t_p = t_s$)

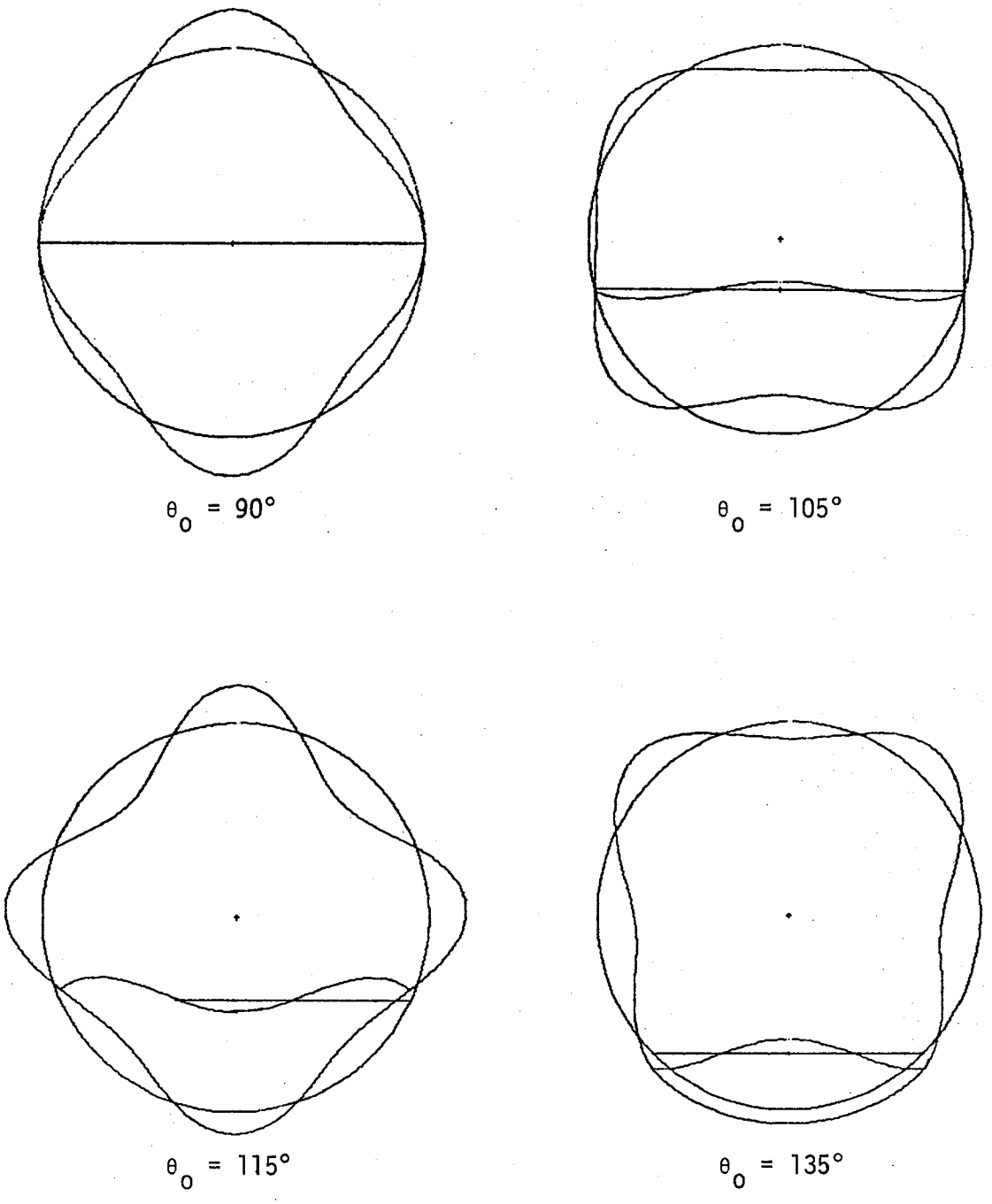

Figure 16. Third Symmetric Mode for Various Plate Locations (Rigid Joint, $t_p = t_s$)

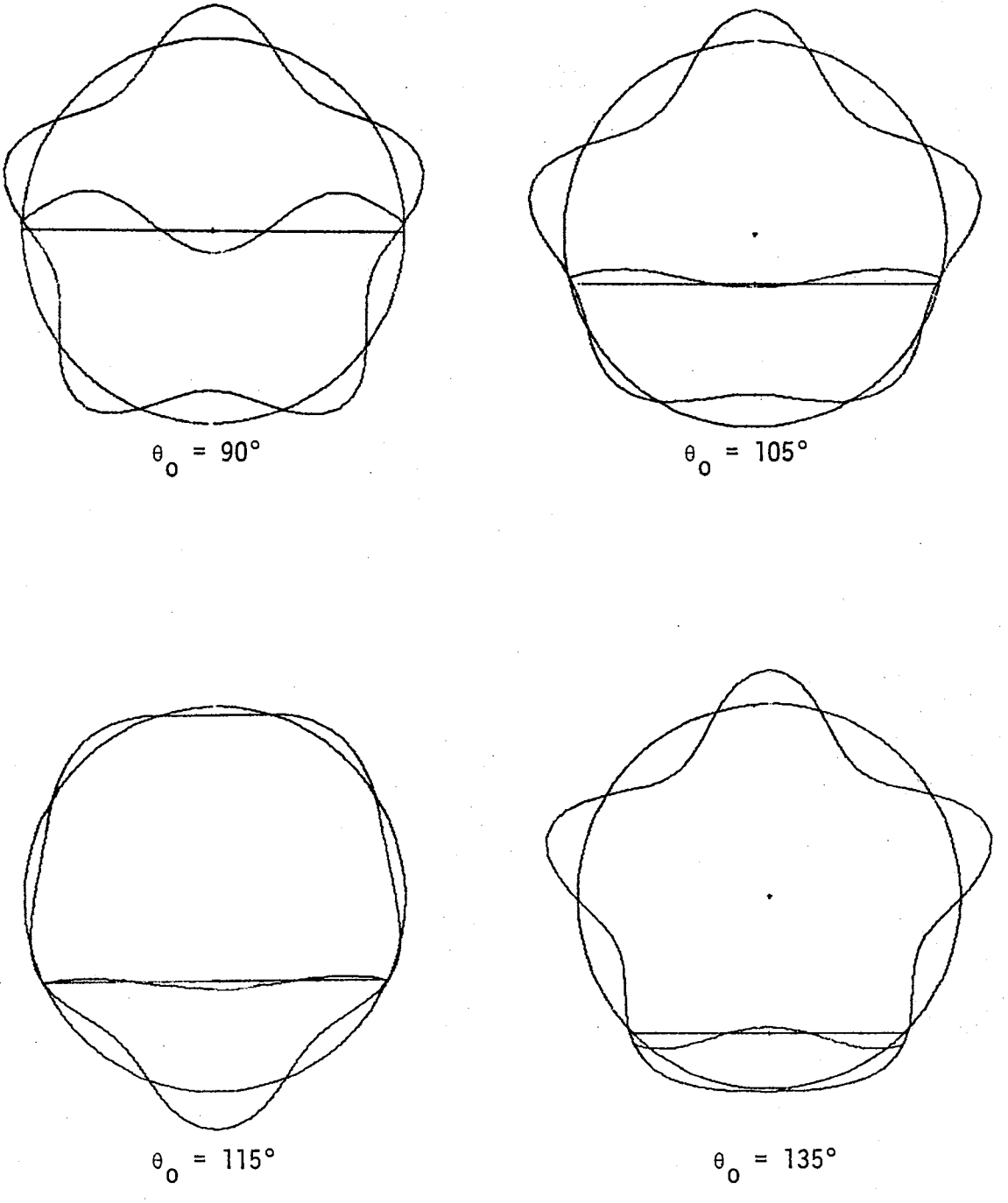

Figure 17. Fourth Symmetric Mode for Various Plate Locations (Rigid Joint, $t_p = t_s$)

The fundamental frequency of a shell with a hinged joint increases as the plate is located farther from the center, as shown by Figure 18. Since this mode involves only bending of the plate, this increase can be attributed to the decrease in width of the plate. The fundamental mode for the case of a rigid joint exhibits principally plate bending, so the same observation may be made. However, as shown by Figure 19, the curve of frequency as a function of θ_o tends to level out at large θ_o due to the increased motion of the shell.

The second mode for the case of the rigid joint shows less change in frequency as the location of the plate changes, which is apparently due to the predominance of the shell motion in that mode.

Other modes show more varied behavior as θ_o increases. The amplitude of the plate does not show a uniform trend and the wave number of the plate may change as the location of the plate changes. These changes in the character of some mode shapes as the location of the plate changes may cause the frequencies of that mode to increase or decrease.

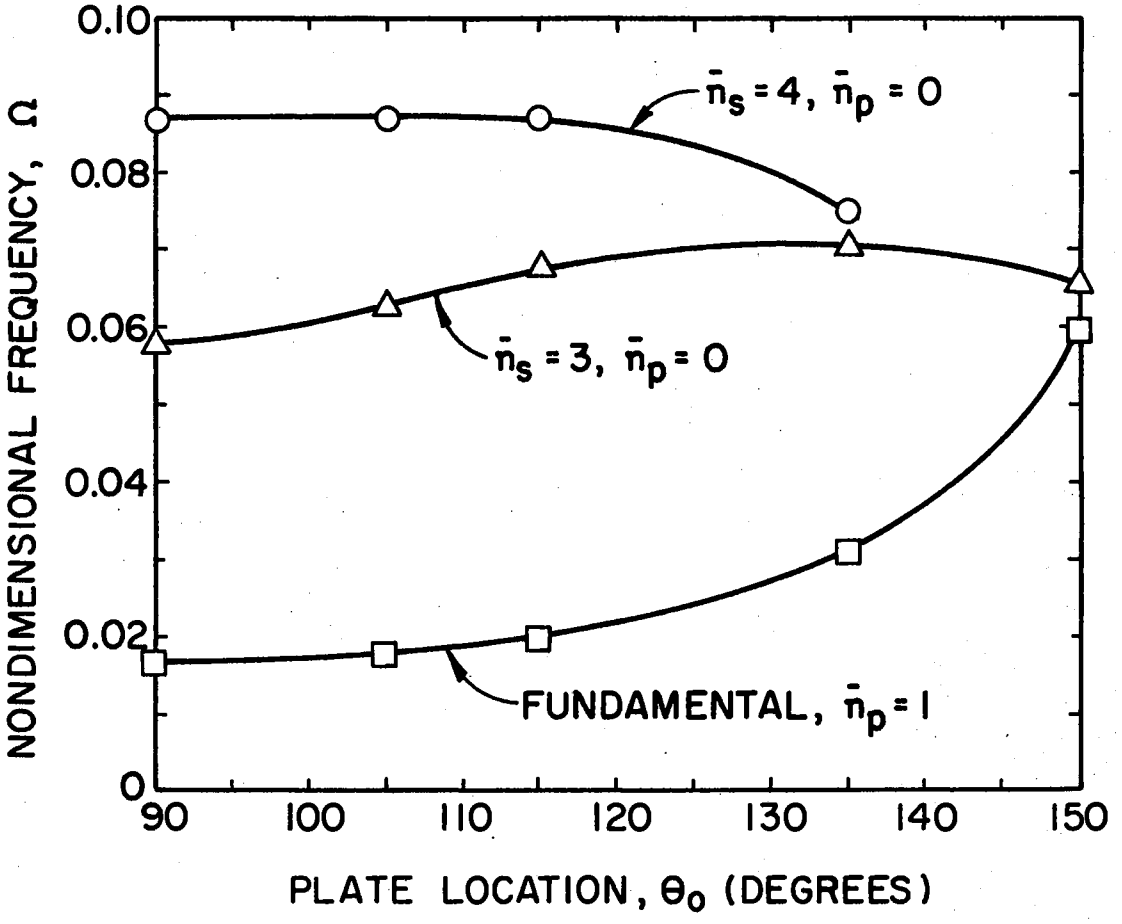

Figure 18. The Effect of the Location of the Plate on the Frequencies of a Shell With a Hinged Joint ($t_p = t_s$, Symmetric Modes)

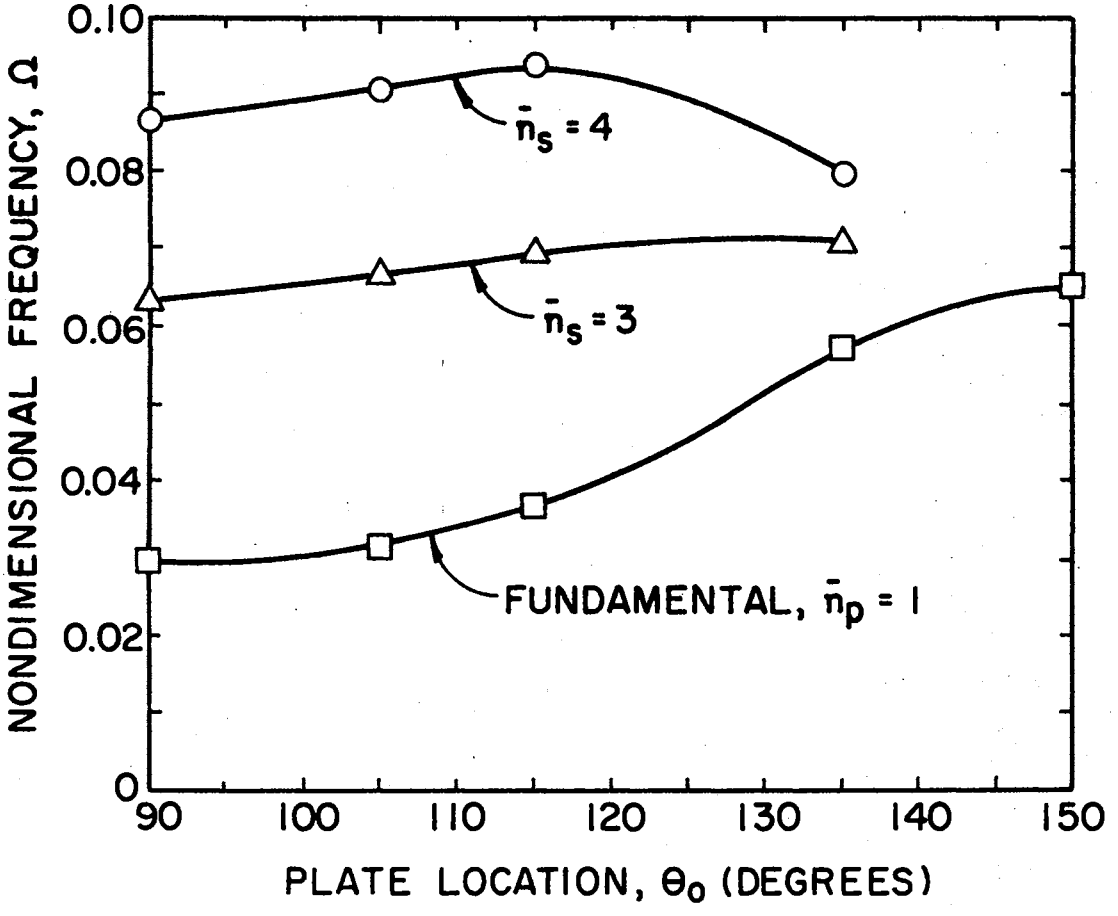

Figure 19. The Effect of the Location of the Plate on the Frequencies of a Shell With a Rigid Joint ($t_p = t_s$, Symmetric Modes)

CHAPTER IV

SUMMARY, CONCLUSIONS AND RECOMMENDATIONS

A method has been developed for free vibration analyses of circular cylindrical shells with single, longitudinal partitioning plates. This method was based on the extended Rayleigh-Ritz technique. Separate displacement functions were assumed for the regions of the shell and plate. Constraint equations were used to enforce compatibility between the regions.

This method was employed for a study of the characteristics of the vibration of partitioned shells. The study considered the following items, for which results have been presented:

1. A study was made to determine the importance of including the in-plane degrees of freedom of the plate in the analysis.

2. Analyses were made to determine how the frequencies and modes of the system differed for two types of joints between the shell and plate. Rigid and hinged joints were considered.

3. The effect of the thickness of the plate on the frequencies and modes of the system was studied.

4. The influence of the position of the partitioning plate on the modes and frequencies of the system was investigated.

The major observations and conclusions from this study are listed below.

1. Neglecting the in-plane degrees of freedom of the plate will cause slight error (less than one percent) in some frequencies and greater errors in others, depending on the extent of the in-plane motion in that mode. It is desirable to include some plate in-plane degrees of freedom in the analysis. Excellent results can be obtained by using only one-half to one-third as many terms in the displacement series for the in-plane directions as are used in the series for the displacement normal to the surface of the plate.

2. When the joint between the shell and plate is hinged, there exist modes of the system, with negligible shell motion, in which the plate vibrates essentially as a simply supported plate. The frequencies of these modes are therefore equal to those of the plate alone. The fundamental mode is of this type if the ratio of plate to shell thickness is not too large (less than about 3.2 for the cases considered here). The deformation of the shell in these modes may become significant if the thickness ratio is very large. The remaining modes exhibit motion of the shell, plate longitudinal bending, and plate in-plane deformation, but no bending of the plate in the transverse direction.

3. For a shell with a hinged joint, an increase in the thickness of the plate causes a slight decrease in the frequencies of those modes involving no transverse plate bending. Therefore, in these modes, the effect of the increase of the inertia of the plate is greater than the effect of its increased stiffness.

4. When the joint between the plate and shell is rigid, some modes of the system involve predominant motion of either the shell or plate. The fundamental mode exhibits principally plate motion with one half wave in each direction, unless the plate is very thick (more than about

three times as thick as the shell, for the cases considered in this study).

5. For the case of a rigid joint, the amplitude of the plate vibration decreases as the thickness of the plate increases. The frequencies become less sensitive to changes in the plate thickness as it increases.

6. The first several mode shapes are very similar for both joint conditions. This indicates that the in-plane restraint of the plate has a greater effect on the shapes of the modes than its bending restraint. For very thick plates, the bending restraint becomes significant.

7. The frequencies of a partitioned shell are higher when the joint is rigid than when it is hinged.

8. The frequencies of modes that involve little or no bending of the plate are relatively insensitive to the joint condition or the thickness of the plate.

9. Frequencies of modes that involve appreciable bending of the plate increase as the thickness of the plate increases. For the case of a hinged joint between the plate and shell, these frequencies vary linearly with the thickness of the plate.

10. If the mode shapes are arranged in order of frequency, the order will change as the thickness of the plate is varied.

11. The fundamental frequency of the system increases as the plate is located farther from the center.

12. For the partitioned shells analyzed in this study, the lowest mode that involves significant shell motion has the same number of circumferential waves as the fundamental mode of an unpartitioned shell.

13. Unlike the unpartitioned shell, the wave numbers of a partitioned shell are not unique. A symmetric and an antisymmetric mode may have the same number of circumferential waves for the shell. Several modes may have the same number of waves for the plate. It is often difficult to assign wave numbers to other than the first few modes.

The following recommendations for further study are made:

1. The results of this method of analysis should be compared with results obtained by other methods of analysis, such as finite difference or finite element methods.

2. Experimental data would be valuable for verification of the results of this study.

3. Other parametric studies should be conducted to determine how the frequencies of the partitioned shell vary with the length and thickness of the shell. Other boundary conditions may be considered.

4. The capability to allow stiffening members for the plate and shell would be of practical importance for aircraft structures. With the present method, stiffened shells and plates can be analyzed only if they can be treated as unstiffened plates and shells with orthotropic properties. Many extensions to this method of analysis can be proposed, such as inclusion of the capability to analyze noncircular cylindrical shells and shells with cutouts.

5. The method of analysis that was used in this study can be extended to allow the computation of the dynamic response of partitioned shells to transient loads. This appears to be an efficient method for solving such problems.

6. A general area in which research seems profitable is the combination of Rayleigh-Ritz analyses, such as this one, with the finite

element method. The Rayleigh-Ritz method could then be used for large uniform areas of a structure, for which it is best suited. Finite elements could be used for regions with complicated geometry, for which they are most efficient. Constraint equations would be used to join the regions.

BIBLIOGRAPHY

(1) Arnold, R. N. and G. B. Warburton. "Flexural Vibrations of the Walls of Thin Cylindrical Shells Having Freely Supported Ends." Proc. Royal Soc. London, Vol. 197A (1949), pp. 238-256.

(2) Kalnins, A. "Dynamic Problems of Elastic Shells." Appl. Mech. Reviews, Vol. 18, No. 11 (November,1965), pp. 867-872.

(3) Bert, C. W. and D. M. Egle. "Dynamics of Composite, Sandwich, and Stiffened Shell-Type Structures." Jour. Spacecraft and Rockets, Vol. 6, No. 12 (December,1969), pp. 1345-1361.

(4) Leissa, A. W. Vibrations of Shells. NASA SP-288, 1973.

(5) Sewall, J. L., W. M. Thompson, and C. G. Pusey. "An Experimental and Analytical Vibration Study of Elliptical Cylindrical Shells." NASA TN D-6089, February,1971.

(6) Egle, D. M. and J. L. Sewall. "An Analysis of Free Vibrations of Orthogonally Stiffened Cylindrical Shells with Stiffeners Treated as Discrete Elements." AIAA Jour., March,1968.

(7) Boyd, D. E. and C. K. P. Rao. "A Theoretical Analysis of the Free Vibrations of Ring and Stringer Stiffened Elliptical Cylinders with Arbitrary End Conditions." NASA CR-2151, February,1973.

(8) Brugh, R. L. "An Evaluation of Analytical Methods Using the Rayleigh-Ritz Approach for the Free Vibrations of Stiffened Noncircular Cylindrical Shells." (Ph.D. thesis, Oklahoma State University, 1973.)

(9) Junger, M. C. "Dynamic Behavior of Reinforced Cylindrical Shells in Vacuum and in a Fluid." Jour. Appl. Mech., Vol. 21 (1954) p. 35.

(10) Basdekas, N. L. and M. Chi. "Response of Oddly-Stiffened Circular Cylindrical Shells." Jour. Sound Vib., Vol. 17, No. 2 (1971), pp. 187-206.

(11) Klein, S. "A Study of the Matrix Displacement Method as Applied to Shells of Revolution." AFFDL-TR-66-80. Proc. of the Conf. on Matrix Methods in Struct. Mech., Wright-Patterson AFB (November,1966), pp. 275-299.

(12) Argyris, J. H. "Continua and Discontinua." AFFDL-TR-66-80. Proc. of the Conf. on Matrix Methods in Struct. Mech., Wright-Patterson AFB (November,1966), pp. 11-189.

(13) Argyris, J. H. and S. Kelsey. Modern Fuselage Analysis and the Elastic Aircraft. London: Butterworths, 1963.

(14) Harari, A. and M. L. Baron. "Discrete Analysis for the Dynamic Response of Stiffened Shells." P. Weidlinger, Consulting Engr. Tech. Rept. No. 10 for ONR Contract N00014-70-C-0359, March,1971.

(15) Soong, T. C. "Buckling of Stiffened Cylindrical Shells of Circular Arc Cross Section." Aeronautical Quar. (August,1970), pp. 263-279.

(16) Hu, W. C. L. and J. P. Raney. "Experimental and Analytical Study of Vibrations of Joined Shells." AIAA Jour., Vol. 5, No. 5 (May,1967), pp. 976-980.

(17) Steeves, E. C., B. J. Durling, and W. C. Walton. "A Method for Computing the Response of a General Axisymmetric Shell With an Attached Asymmetric Structure." Proc. of AIAA Structural Dynamics and Aeroelasticity Specialists Conference, New Orleans, La., 1969, pp. 302-328.

(18) Hurty, W. C. "Dynamic Analysis of Structural Systems Using Component Modes." AIAA Jour., Vol. 3, No. 4 (1965), pp. 678-685.

(19) Budiansky, B. and P. C. Hu. "The Lagrangian Multiplier Method of Finding Upper and Lower Limits to Critical Stresses of Clamped Plates." NACA TN-1103, 1946.

(20) Budiansky, B., P. C. Hu, and R. W. Conner. "Notes on the Lagrangian Multiplier Method in Elastic Stability Analysis." NACA TN-1558, 1948.

(21) Webster, J. J. "Free Vibration Analysis of Structures Using Rayleigh-Ritz and Finite Element Methods." Proc. of the Symposium on Structural Dynamics, Loughborough Univ. of Technology, Leics., England, March,1970 (IAA A70-25055).

(22) Webster, J. J. "Free Vibrations of Rectangular Curved Panels." Int. Jour. Mech. Sci., Vol. 10 (1968), pp. 571-582.

(23) IBM System 360 Scientific Subroutine Package Version III Programmer's Manual, International Business Machines Corp., 1968.

(24) Kraus, H. Thin Elastic Shells. New York: John Wiley and Sons, 1967.

(25) Leissa, A. W. Vibrations of Plates. NASA SP-160, 1969.

(26) Felgar, R. P., Jr. "Formulas for Integrals Containing Characteristic Functions of a Vibrating Beam." Circular No. 14, Bureau of Eng. Res., Univ. of Texas, 1950.

(27) Chang, T. and R. R. Craig, Jr. "On Normal Modes of Uniform Beams." Engr. Mech. Res. Lab, Univ. of Texas at Austin, Report EMRL 1068, January,1969.

(28) Wilkinson, J. H. The Algebraic Eigenvalue Problem. Oxford: Clarendon Press, 1965, p. 337.

APPENDIX A

SHELL MASS AND STIFFNESS MATRICES

The general expressions for the mass and stiffness matrices are presented in Chapter II. The details of the development are presented here.

Shell theory enters into the analysis through the strain-displacement relations. In this analysis, Love's first approximation theory is used to reduce the elastic shell problem to a two dimensional problem (24).

A vector of stress resultants for the shell is defined as:

$$\{\sigma_s\} = \begin{Bmatrix} N_x \\ N_\theta \\ N_{x\theta} \\ M_x \\ M_\theta \\ M_{x\theta} \end{Bmatrix}_s \tag{A.1}$$

In this vector, N_x and N_θ are resultants of the normal stresses, $N_{x\theta}$ is a shearing stress resultant, M_x and M_θ are bending stress resultants, and $M_{x\theta}$ is a torsional stress resultant. A vector of mid-surface generalized strains is also defined in Love's theory:

$$\{\varepsilon_s\} = \begin{Bmatrix} \varepsilon_x \\ \varepsilon_\theta \\ \varepsilon_{x\theta} \\ \kappa_x \\ \kappa_\theta \\ \kappa_{x\theta} \end{Bmatrix}_s \tag{A.2}$$

where ε_x and ε_θ are normal strains, $\varepsilon_{x\theta}$ is a shearing strain, κ_x and κ_θ are curvature changes, and $\kappa_{x\theta}$ is the twist. The mid-surface displacements in the three coordinate directions are

$$\{\tilde{u}_s\} = \begin{Bmatrix} u_s \\ v_s \\ w_s \end{Bmatrix} \tag{A.3}$$

The matrix form of the strain-displacement relations of Love's theory is

$$\{\varepsilon_s\} = [G_s]\ \{\tilde{u}_s\}, \tag{A.4}$$

in which

$$[G_s] = \begin{bmatrix} \frac{\partial}{\partial x} & 0 & 0 \\ 0 & \frac{1}{r}\frac{\partial}{\partial \theta} & \frac{1}{r} \\ \frac{1}{r}\frac{\partial}{\partial \theta} & \frac{\partial}{\partial x} & 0 \\ 0 & 0 & -\frac{\partial^2}{\partial x^2} \\ 0 & \frac{1}{r^2}\frac{\partial}{\partial \theta} & -\frac{1}{r^2}\frac{\partial^2}{\partial \theta^2} \\ & \frac{1}{r}\frac{\partial}{\partial x} & -\frac{2}{r}\frac{\partial^2}{\partial x \partial \theta} \end{bmatrix} \tag{A.5}$$

The orthotropic stress-strain relations for these stress resultants and generalized strains are

$$\{\sigma_s\} = [D]\ \{\varepsilon_s\}, \tag{A.6}$$

where the matrix [D] depends on the material properties:

$$[D] = \begin{bmatrix} K_x & \nu_x K_\theta & 0 & 0 & 0 & 0 \\ \nu_\theta K_x & K_\theta & 0 & 0 & 0 & 0 \\ 0 & 0 & G_{x\theta}t & 0 & 0 & 0 \\ 0 & 0 & 0 & D_x & \nu_x D_\theta & 0 \\ 0 & 0 & 0 & \nu_\theta D_x & D_\theta & 0 \\ 0 & 0 & 0 & 0 & 0 & \frac{G_{x\theta}t^3}{12} \end{bmatrix} \tag{A.7}$$

in which

$$K_x = \frac{E_x t}{(1-\nu_x\nu_\theta)}, \quad K_\theta = \frac{E_\theta t}{(1-\nu_x\nu_\theta)},$$

$$D_x = \frac{K_x t^2}{12}, \text{ and } D_\theta = \frac{K_\theta t^2}{12}.$$

To develop the mass and stiffness matrices, the matrix [N], which defines the transformation $\{u_s\} = [N_s]\ \{q_s\}$ between the physical displacements and the generalized coordinates, is required. It is obtained by writing the displacement function series of Equation (2.26) in matrix form:

$$\{u_s\} = \left[\begin{array}{ccc|ccc|ccc} \phi_1\psi_{u1} & \cdots & \phi_{m^*}\psi_{un^*} & 0 & \cdots & 0 & 0 & \cdots & 0 \\ 0 & \cdots & 0 & \phi_1\psi_{v1} & \cdots & \phi_{m^*}\psi_{vn^*} & 0 & \cdots & 0 \\ 0 & \cdots & 0 & 0 & \cdots & 0 & \phi_1\psi_{w1} & \cdots & \phi_{m^*}\psi_{wn^*} \end{array}\right] \begin{Bmatrix} \bar{u}_s \\ \bar{v}_s \\ \bar{w}_s \end{Bmatrix} \tag{A.8}$$

The mass matrix is then given by Equation (2.13):

$$[M_s] = \int_S \rho [N_s]^T [N_s] dS.$$

In terms of the functions in matrix $[N_s]$, the mass matrix is

$$[M_s] = \begin{bmatrix} (MSUU) & 0 & 0 \\ 0 & (MSVV) & 0 \\ 0 & 0 & (MSWW) \end{bmatrix} \tag{A.9}$$

The elements of each submatrix of $[M_s]$ are

$$(MSUU)_{ij} = \int_S \int \phi'_{m_i} \phi'_{m_j} \psi_{un_i} \psi_{un_j} \, R dx d\theta$$

$$(MSVV)_{ij} = \int_S \int \phi_{m_i} \phi_{m_j} \psi_{vn_i} \psi_{vn_j} \, R dx d\theta$$

$$(MSWW)_{ij} = \int_S \int \phi_{m_i} \phi_{m_j} \psi_{wn_i} \psi_{wn_j} \, R dx d\theta,$$

where m_i and n_i are the m and n of the i^{th} term in the generalized coordinate vectors defined in Equation (2.4) and m_j and n_j are the m and n corresponding to the j^{th} term. It is convenient to label each of the different integrals appearing in the mass and stiffness matrices. These integrals are presented in Appendix C. The elements of the submatrices of $[M_s]$ can then be written as

$$\begin{aligned} (MSUU)_{ij} &= \rho R I_3 J_1 \\ (MSVV)_{ij} &= \rho R I_1 J_6 \\ (MSWW)_{ij} &= \rho R I_1 J_{11}, \end{aligned} \tag{A.10}$$

where the integrals of longitudinal functions are labeled I and those of the circumferential functions are designated J.

The stiffness matrix is given by Equation (2.11), which is

$$[K_s] = \int_S [B_s]^T [D] [B_s] \, dS$$

where

$$[B_s] = [G_s]\,[N_s].$$

By using $[G_s]$ from Equation (A.5), $[N_s]$ from Equation (A.8) and $[D]$ from Equation (A.7) in Equation (2.11), the elements of $[K_s]$ can be expressed as follows:

$$[K_s] = \begin{bmatrix} (KSUU) & (KSUV) & (KSUW) \\ (KSUV)^T & (KSVV) & (KSVW) \\ (KSUW)^T & (KSVW)^T & (KSWW) \end{bmatrix} \tag{A.11}$$

The elements of each $\bar{\bar{N}}\bar{\bar{M}}$ x $\bar{\bar{N}}\bar{\bar{M}}$ submatrix are as follows:

$$(KSUU)_{ij} = RK_x I_4 J_1 + G_{x\theta}\frac{t^3}{R}\, I_3 J_2$$

$$(KSUV)_{ij} = \nu_x K_\theta I_5 J_3 + G_{x\theta} t\, I_3 J_4$$

$$(KSUW)_{ij} = \nu_x K_\theta I_5 J_5$$

$$(KSVV)_{ij} = \left(\frac{K_\theta}{R} + \frac{D_\theta}{R^3}\right) I_1 J_7 + \left(R + \frac{t^2}{12R}\right) G_{x\theta} t\, I_3 J_6$$

$$(KSVW)_{ij} = \frac{K_\theta}{R}\, I_1 J_9 - \frac{D_\theta}{R^3}\, I_1 J_{10} - \frac{\nu_\theta D_x}{R}\, I_2 J_9 - \frac{G_{x\theta} t^3}{6R}\, I_3 J_8$$

$$(KSWW)_{ij} = \frac{K_\theta}{R}\, I_1 J_{11} + D_x R I_4 J_{11} + \frac{\nu_x D_\theta}{R}\, I_5 J_{13} + \frac{D_\theta}{R^3}\, I_1 J_{14}$$

$$+ \frac{\nu_\theta D_x}{R}\, I_2 J_{15} + \frac{G_{x\theta} t^3}{3R}\, I_3 J_{12}.$$

APPENDIX B

PLATE MASS AND STIFFNESS MATRICES

The development of the plate mass and stiffness matrices is completely analogous to that in Appendix A for the shell matrices, except that the strain-displacement relations are derived from plate theory (25).

The stress resultants and generalized strains for the plate are defined in the same way as for the shell:

$$\{\sigma_p\} = \begin{Bmatrix} N_x \\ N_y \\ N_{xy} \\ M_x \\ M_y \\ M_{xy} \end{Bmatrix}_p \qquad \{\epsilon_p\} = \begin{Bmatrix} \epsilon_x \\ \epsilon_y \\ \epsilon_{xy} \\ \kappa_x \\ \kappa_y \\ \kappa_{xy} \end{Bmatrix}_p \tag{B.1}$$

The mid-surface displacements are denoted by

$$\{\tilde{u}_p\} = \begin{Bmatrix} u_p \\ v_p \\ w_p \end{Bmatrix} \tag{B.2}$$

The strain displacement relations of plate theory are

$$\{\epsilon_p\} = [G_p]\ \{\tilde{u}_p\} \tag{B.3}$$

where

$$[G_p] = \begin{bmatrix} \frac{\partial}{\partial x} & & 0 \\ 0 & \frac{\partial}{\partial y} & 0 \\ \frac{\partial}{\partial y} & \frac{\partial}{\partial x} & 0 \\ 0 & 0 & -\frac{\partial^2}{\partial x^2} \\ 0 & 0 & -\frac{\partial^2}{\partial y^2} \\ 0 & 0 & -2\frac{\partial^2}{\partial x \partial y} \end{bmatrix} \tag{B.4}$$

The stress-strain relation for the plate is:

$$\{\sigma_p\} = [D]\ \{\varepsilon_p\} \tag{B.5}$$

where [D] is the same as the [D] in Equation (A.7) if the subscript θ in Equation (A.7) is replaced by y.

The transformation matrix $[N_p]$ is of exactly the same form as $[N_s]$, with the plate transverse functions in place of the shell circumferential functions.

The plate mass matrix is then obtained from

$$[M_p] = \int_S \rho [N_p]^T [N_p]\ dS. \tag{B.6}$$

The resulting matrix has the following form:

$$[M_p] = \begin{bmatrix} (MPUU) & 0 & 0 \\ 0 & (MPVV) & 0 \\ 0 & 0 & (MPWW) \end{bmatrix} \tag{B.7}$$

The elements of the submatrices are:

$$(MPUU)_{ij} = \rho I_3 H_1$$
$$(MPVV)_{ij} = \rho I_1 H_6 \qquad (B.8)$$
$$(MPWW)_{ij} = \rho I_1 H_7$$

where I denotes an integral of the longitudinal functions and H designates an integral of the plate transverse functions. These integrals are presented in Appendix C.

The plate stiffness matrix is defined by

$$[K_p] = \int_S [B_p]^T [D] [B_p] \, dS, \quad \text{where } [B_p] = [G_p] [N_p] \qquad (B.9)$$

The stiffness matrix has the following form:

$$[K_p] = \begin{bmatrix} (KPUU) & (KPUV) & 0 \\ (KPUV)^T & (KPVV) & 0 \\ 0 & 0 & (KPWW) \end{bmatrix} \qquad (B.10)$$

The elements of the submatrices in Equation (B.10) are as follows:

$$(KPUU)_{ij} = K_x I_4 H_1 + G_{xy} t \, I_3 H_4$$
$$(KPUV)_{ij} = \nu_x K_y I_5 H_2 + G_{xy} t \, I_3 H_5$$
$$(KPVV)_{ij} = K_y I_1 H_3 + G_{xy} t \, I_3 H_6$$
$$(KPWW)_{ij} = D_x I_4 H_7 + \nu_y D_x I_2 H_{11} + D_y I_1 H_9 + \nu_x D_y I_5 H_8 + \frac{G_{xy} t^3}{3} I_3 H_{10}.$$

APPENDIX C

INTEGRALS OF THE FUNCTIONS IN THE ASSUMED DISPLACEMENT SERIES

This appendix contains the expressions for the integrals appearing in the mass and stiffness matrix elements given in Appendixes A and B.

The integrals of the longitudinal functions for the plate and shell are as follows:

$$I_1 = \int_o^L \phi_j \, \phi_k \, dx$$

$$I_2 = \int_o^L \phi_j'' \, \phi_k \, dx$$

$$I_3 = \int_o^L \phi_j' \, \phi_k' \, dx$$

$$I_4 = \int_o^L \phi_j'' \, \phi_k'' \, dx$$

$$I_5 = \int_o^L \phi_j \, \phi_k''' \, dx.$$

Closed-form expressions for these integrals, for the functions ϕ used in this analysis, have been tabulated by Felgar (26).

The integrals of the circumferential functions used in the displacement series for the shell are:

$$J_1 = \int_o^{2\pi} \psi_{uj} \, \psi_{uk} \, d\theta$$

$$J_2 = \int_o^{2\pi} \psi_{uj}' \, \psi_{uk}' \, d\theta$$

$$J_3 = \int_o^{2\pi} \psi_{vj}' \, \psi_{uk} \, d\theta$$

$$J_4 = \int_o^{2\pi} \psi_{vj}\, \psi'_{uk}\, d\theta$$

$$J_5 = \int_o^{2\pi} \psi_{wj}\, \psi_{uk}\, d\theta$$

$$J_6 = \int_o^{2\pi} \psi_{vj}\, \psi_{vk}\, d\theta$$

$$J_7 = \int_o^{2\pi} \psi'_{vj}\, \psi'_{vk}\, d\theta$$

$$J_8 = \int_o^{2\pi} \psi'_{wj}\, \psi_{vk}\, d\theta$$

$$J_9 = \int_o^{2\pi} \psi_{wj}\, \psi'_{vk}\, d\theta$$

$$J_{10} = \int_o^{2\pi} \psi''_{wj}\, \psi'_{vk}\, d\theta$$

$$J_{11} = \int_o^{2\pi} \psi_{wj}\, \psi_{wk}\, d\theta$$

$$J_{12} = \int_o^{2\pi} \psi'_{wj}\, \psi'_{wk}\, d\theta$$

$$J_{13} = \int_o^{2\pi} \psi''_{wj}\, \psi_{wk}\, d\theta$$

$$J_{14} = \int_o^{2\pi} \psi''_{wj}\, \psi''_{wk}\, d\theta$$

$$J_{15} = \int_o^{2\pi} \psi_{wj}\, \psi''_{wk}\, d\theta$$

The integrals of the plate transverse functions are defined as follows:

$$H_1 = \int_{-b}^{b} \xi_{uj}\, \xi_{uk}\, dy$$

$$H_2 = \int_{-b}^{b} \xi'_{vj}\, \xi_{uk}\, dy$$

$$H_3 = \int_{-b}^{b} \xi'_{vj}\, \xi'_{vk}\, dy$$

$$H_4 = \int_{-b}^{b} \xi'_{uj}\, \xi'_{uk}\, dy$$

$$H_5 = \int_{-b}^{b} \xi_{vj} \, \xi'_{uk} \, dy$$

$$H_6 = \int_{-b}^{b} \xi_{vj} \, \xi_{vk} \, dy$$

$$H_7 = \int_{-b}^{b} \xi_{wj} \, \xi_{wk} \, dy$$

$$H_8 = \int_{-b}^{b} \xi''_{wj} \, \xi_{wk} \, dy$$

$$H_9 = \int_{-b}^{b} \xi''_{wj} \, \xi''_{wk} \, dy$$

$$H_{10} = \int_{-b}^{b} \xi'_{wj} \, \xi'_{wk} \, dy$$

$$H_{11} = \int_{-b}^{b} \xi_{wj} \, \xi''_{wk} \, dy.$$

APPENDIX D

BEAM MODE FUNCTIONS

The characteristic modes of vibration of a uniform beam are used for the longitudinal functions in the assumed displacement series. These functions are listed below. They are described in detail by Chang and Craig (27).

For a simply supported beam, the mode functions are

$$\phi_m(x) = \sin \frac{m\pi x}{L} .$$

The mode functions for a clamped-clamped beam are

$$\phi_m(x) = [\cosh (\beta_m x) - \cos (\beta_m x)] - \alpha_m[\sinh (\beta_m x) - \sin (\beta_m x)]$$

where

$$\alpha_m = \frac{\cosh(\beta_m L) - \cos(\beta_m L)}{\sinh(\beta_m L) - \sin(\beta_m L)}$$

and β_m is the m^{th} root of the transcendental equation:

$$\cos (\beta L) \cosh (\beta L) = 1.$$

The values of α_m and β_m are tabulated in Reference (27).

For a clamped-free beam, the mode functions are

$$\phi_m(x) = [\cosh (\beta_m x) - \cos (\beta_m x)] - \alpha_m[\sinh (\beta_m x) - \sin (\beta_m x)]$$

in which β_m is the m^{th} root of

$$\cos (\beta L) \cosh (\beta L) = -1$$

and

$$\alpha_m = \frac{\cosh(\beta_m L) + \cos(\beta_m L)}{\sinh(\beta_m L) + \sin(\beta_m L)}$$

The mode functions for a free-free beam, excluding rigid body modes, are given by

$$\phi_m(x) = [\cosh(\beta_m x) + \cos(\beta_m x)] - \alpha_m[\sinh(\beta_m x) + \sin(\beta_m x)]$$

where β_m is determined from

$$\cos(\beta L)\cosh(\beta L) = 1$$

and

$$\alpha_m = \frac{\cos(\beta_m L) - \cosh(\beta_m L)}{\sin(\beta_m L) - \sinh(\beta_m L)} .$$

APPENDIX E

COMPATIBILITY AND CONSTRAINT EQUATIONS

The plate and shell are both defined only in terms of their middle surfaces, so the joint between them is a line formed by the intersection of their middle surfaces.

The displacement compatibility equations are derived by equating the shell and plate displacements at the joint. All displacements must be expressed in the same coordinate system in order to do this, so the shell displacements will be transformed to the plate coordinate system. The shell displacements at the joint are referred to coordinate axes normal and tangential to the shell surface at the joint (see Figure 1), so the transformation involves a rotation of coordinates about the x axis through the angle θ_o. Transforming the shell displacement vector by premultiplying by a coordinate rotation matrix and equating to the plate displacements yields:

$$\begin{bmatrix} 1 & 0 & 0 \\ 0 & \cos\theta_o & -\sin\theta_o \\ 0 & \sin\theta_o & \cos\theta_o \end{bmatrix} \begin{Bmatrix} u_s \\ v_s \\ w_s \end{Bmatrix} = \begin{Bmatrix} u_p \\ v_p \\ w_p \end{Bmatrix}$$

This is the matrix form of the displacement compatibility equations. They can be written individually as

$$u_s = u_p \tag{E.1a}$$

$$v_s \cos\theta_o - w_s \sin\theta_o = v_p \tag{E.1b}$$

$$v_s \sin\theta_o + w_s \cos\theta_o = w_p \tag{E.1c}$$

Compatibility of the rotations of the plate and shell at the joint must also be considered. The rotations of an element of the edge of the plate about each of the plate coordinate axes are

$$\begin{aligned} \phi_x^p &= \frac{\partial w_p}{\partial y} \\ \phi_y^p &= -\frac{\partial w_p}{\partial x} \\ \phi_z^p &= \frac{\partial v_p}{\partial x} \end{aligned} \tag{E.2}$$

The rotations of an element of the joint line on the shell about each of the shell coordinate directions at the joint are

$$\begin{aligned} \phi_x^s &= \frac{1}{r}\frac{\partial w_s}{\partial \theta} - \frac{v_s}{r} \\ \phi_\theta^s &= -\frac{\partial w_s}{\partial x} \\ \phi_z^s &= \frac{\partial v_s}{\partial x} \end{aligned} \tag{E.3}$$

Transforming the shell rotations into the plate coordinate system and equating the result to the plate rotations yields the following rotation compatibility equations:

$$\begin{aligned} \phi_x^s &= \phi_x^p \\ \phi_\theta^s \cos\theta_o - \phi_z^s \sin\theta_o &= \phi_y^p \\ \phi_\theta^s \sin\theta_o + \phi_z^s \cos\theta_o &= \phi_z^p. \end{aligned} \tag{E.4}$$

Substitution of Equations (E.2) and (E.3) into Equations (E.4) results in the rotation compatibility equations in terms of the displacements.

$$\frac{1}{r}\frac{\partial w_s}{\partial \theta} - \frac{v_s}{r} = \frac{\partial w_p}{\partial y} \tag{E.5a}$$

$$\frac{-\partial w_s}{\partial x}\cos\theta_o - \frac{\partial v_s}{\partial x}\sin\theta_o = -\frac{\partial w_p}{\partial x} \tag{E.5b}$$

$$\frac{-\partial w_s}{\partial x}\sin\theta_o + \frac{\partial v_s}{\partial x}\cos\theta_o = \frac{\partial v_p}{\partial x} \tag{E.5c}$$

Each of the terms in Equations (E.1) and (E.5) is evaluated at the θ or y coordinate of the joint, but still remains a function of x. If displacement compatibility is required by Equations (E.1), then Equations (E.5b) and (E.5c) are also satisfied. This may be verified by substituting v_p and w_p from Equations (E.1b) and (E.1c) into them. Hence, four equations are needed to enforce compatibility of all displacements and rotations, Equations (E.1) and (E.5a).

In order to obtain the constraint equations in terms of the generalized coordinates, the displacement functions of Equation (2.27) are substituted for the displacements in Equations (E.1) and (E.5a). This yields Equation (2.35).

The constraint matrix is formulated by writing Equation (2.35) in matrix form. The constraint matrix for a rigid joint between the shell and plate has $4\bar{M}$ rows and $6\bar{M}\bar{N}$ columns (see Equation (E.6) below).

The elements of the submatrices are listed below, where [I] is an identity matrix of order $\bar{M}$.

$$[C1]_n = \psi_{un}(\theta_o)\ [I]$$

$$[C2]_n = \psi_{vn}(\theta_o)\cos\theta_o\ [I]$$

$$[C3]_n = -\psi_{wn}(\theta_o)\sin\theta_o\ [I]$$

$$[C4]_n = \psi_{vn}(\theta_o)\sin\theta_o\ [I]$$

$$[C5]_n = \psi_{wn}(\theta_o)\cos\theta_o\ [I]$$

$$
\begin{bmatrix}
[C1]_0 \ldots [C1]_{n^*} & & & [C8]_0 \ldots [C8]_{n^*} & & \\
\hline
 & [C2]_0 \ldots [C2]_{n^*} & [C3]_0 \ldots [C3]_{n^*} & & [C9]_0 \ldots [C9]_{n^*} & \\
\hline
 & [C4]_0 \ldots [C4]_{n^*} & [C5]_0 \ldots [C5]_{n^*} & & & [C10]_0 \ldots [C10]_{n^*} \\
\hline
 & [C6]_0 \ldots [C6]_{n^*} & [C7]_0 \ldots [C7]_{n^*} & & & [C11]_0 \ldots [C11]_{n^*}
\end{bmatrix}
\begin{Bmatrix}
\bar{u}_s \\ \bar{v}_s \\ \bar{w}_s \\ \bar{u}_p \\ \bar{v}_p \\ \bar{w}_p
\end{Bmatrix}
= \{0\}
\qquad \text{(E.6)}
$$

$$[C6]_n = \frac{1}{r} \psi_{vn}(\theta_o) \; [I]$$

$$[C7]_n = -\frac{1}{r} \frac{\partial \psi_{wn}}{\partial \theta} (\theta_o) \; [I]$$

$$[C8]_n = -\xi_{un}(y_o) \; [I]$$

$$[C9]_n = -\xi_{vn}(y_o) \; [I]$$

$$[C10]_n = -\xi_{wn}(y_o) \; [I]$$

$$[C11]_n = -\frac{\partial \xi_{wn}}{\partial y} (y_o) \; [I].$$

The last $\bar{M}$ rows of the constraint matrix express equality of the rotations about the line of the joint between the plate and shell. The constraint matrix for the case of a hinged joint is obtained by omitting the last row of submatrices of the matrix in Equation (E.6).

APPENDIX F

METHOD OF SOLUTION FOR EIGENVALUES AND EIGENVECTORS

The eigenvalue problem is of the form

$$[K]\{q\} = \lambda[M]\{q\} \tag{F.1}$$

where λ is an eigenvalue, and $\{q\}$ an eigenvector.

The following method for solving for the eigenvectors of the system requires [M] to be positive definite and relies on the fact that [M] and [K] are symmetric (28).

The matrix [M] is decomposed into two triangular factors by the Cholesky decomposition method:

$[M] = [L]\,[L]^T$ where [L] is a lower triangular matrix.

Therefore, from Equation (F.1):

$$[K]\{q\} = \lambda[L][L^T]\{q\}.$$

This can be expressed as

$$[L]^{-1}\,[K]\,[L^T]^{-1}\,[L^T]\{q\} = \lambda[L^T]\{q\}. \tag{F.2}$$

By defining

$$[s] = [L]^{-1}\,[k]\,[L^T]^{-1} \tag{F.3}$$

and

$$\{y\} = [L^T]\{q\}, \tag{F.4}$$

Equation (F.2) becomes

$$[s]\ \{y\} = \lambda\{y\} \tag{F.5}$$

which is an eigenvalue problem in the usual form, where [s] is a symmetric matrix with eigenvalues λ which are the same as the original problem. The eigenvectors of the original system, {q}, are found from the eigenvectors of Equation (F.5), {y}, by Equation (F.4).

Because the transformation of Equation (F.3) involves triangular matrices, the matrix $[L]^{-1}$ need not be found to determine [s]. Thus, no matrix inversions are required. The sequence of operations is as follows:

1. Decompose [M]: $[M] = [L]\ [L^T]$.
2. Perform a forward substitution through
   $$[L]\ ([L]^{-1}\ [K]) = [K]$$
   to solve for each column of $[L]^{-1}\ [K]$.
3. Perform a forward substitution through
   $$L([L]^{-1}\ [K]\ [L^T]^{-1}) = ([L]^{-1}\ [K])^T$$
   to solve for each column of $[L]^{-1}\ [K]\ [L^T]^{-1} = [s]$.
4. Find the eigenvalues, λ, and eigenvectors {y} of [s].
   A Jacobi method was used in this analysis.
5. Determine the eigenvectors {q} from {y} by a back substitution through
   $$[L^T]\ \{q\} = \{y\}.$$

The subroutine that was written to carry out this procedure used library subroutines for steps one and four (23).

VITA \

Michael Ralph Peterson

Candidate for the Degree of

Doctor of Philosophy

Thesis: A STUDY OF THE EFFECTS OF A LONGITUDINAL, INTERIOR PLATE ON THE FREE VIBRATIONS OF CIRCULAR CYLINDRICAL SHELLS

Major Field: Mechanical Engineering

Biographical:

Personal Data: Born November 2, 1944 in Casper, Wyoming, the son of Mr. and Mrs. R. L. Peterson.

Education: Graduated from Sandia High School, Albuquerque, New Mexico, in June, 1962; received the degree of Bachelor of Science in Mechanical Engineering in 1967 and the Master of Science degree in 1969 from the University of New Mexico; completed the requirements for the degree of Doctor of Philosophy in December, 1973.

Professional Experience: Engineering Assistant, Edgerton, Germeshausen, and Grier, Inc., summer of 1966; Assistant Engineer, Eastman Kodak Company, summer of 1967; Graduate Teaching Assistant, University of New Mexico, 1967-1968; Development Engineer, Eastman Kodak Company, 1968-1970; Graduate Teaching Assistant, Oklahoma State University, 1970-1973.

Professional Organizations: Associate Member of the American Society of Mechanical Engineers; Associate Member of the National Society of Professional Engineers; Pi Tau Sigma.